Review

Iron Oxide Nanoparticles: Green Synthesis and their Antimicrobial Activity

Johana Zúñiga-Miranda , Julio Guerra , Alexander Mueller , Arianna Mayorga-Ramos , Saskya E. Carrera-Pacheco , Carlos Barba-Ostria , Jorge Heredia-Moya , Linda P. Guamán *

Posted Date: 3 October 2023

doi: 10.20944/preprints202310.0123.v1

Keywords: antimicrobial resistance; green synthesis; IONPs; antibacterial activity; antifungal activity; antiparasitic; antiviral activity

Review

Iron Oxide Nanoparticles: Green Synthesis and Their Antimicrobial Activity

Johana Zúñiga-Miranda [1], Julio Guerra [2], Alexander Mueller [3], Arianna Mayorga-Ramos [1], Saskya E. Carrera-Pacheco [1], Carlos Barba-Ostria [4], Jorge Heredia-Moya [1] and Linda P. Guamán [1]*.

[1] Centro de Investigación Biomédica (CENBIO), Facultad de Ciencias de la Salud Eugenio Espejo, Universidad UTE, Quito 170527, Ecuador; johana.zuniga@ute.edu.ec (J.Z.-M.); arianna.mayorga@ute.edu.ec (A.M.-R.); saskya.carrera@ute.edu.ec (S.E.C.-P.); jorgeh.heredia@ute.edu.ec (J.H.-M.); linda.guaman@ute.edu.ec (L.P.-G).

[2] Universidad Técnica del Norte; jeguerra@utn.edu.ec (J.G)

[3] Department of Molecular Biology, Princeton University, Princeton, NJ 08544, USA; amm9@princeton.edu (A.M.)

[4] Escuela de Medicina, Colegio de Ciencias de la Salud Quito, Universidad San Francisco de Quito USFQ, Quito 170901, Ecuador; cbarbao@usfq.edu.ec (C.B.-O)

* Correspondence: linda.guaman@ute.edu.ec (L.P.-G)

Abstract: Pathogenic microorganisms can cause a range of infectious diseases and are often treated with antimicrobial agents. The rise of antimicrobial resistance caused by inappropriate use of these agents in various settings has become a global health threat. There is, therefore, a need to find new and effective agents to combat infections caused by resistant pathogens. Nanotechnology has seen significant growth and development in recent years and has a wide range of applications in various fields, including health, agriculture, and industry. This novel area offers the potential for the synthesis of nanoparticles (NPs) with antimicrobial activity, such as iron oxide nanoparticles (IONPs). The use of IONPs is a promising way to overcome antimicrobial resistance or pathogenicity because of their ability to interact with several biological molecules and to inhibit microbial growth. This review focuses on the most common green synthesis methods for producing IONPs using bacteria, fungi, plants, and organic waste, as well as the most common methods for the characterization of these IONPs. Finally, it summarizes their application as promising antibacterial, antifungal, antiparasitic, and antiviral agents.

Keywords: antimicrobial resistance; green synthesis; IONPs; antibacterial activity; antifungal activity; antiparasitic; antiviral activity

1. Introduction

Microbial agents such as fungi, bacteria, parasites, and viruses cause various infectious diseases and can be treated with antimicrobial agents. The main concern in treating infectious diseases is that many pathogenic microorganisms have developed resistance against antimicrobial agents, for example, antibiotics [1]. The development of antibiotic resistance is the result of the inappropriate use of antibiotics in community, clinical, and agricultural settings. Consequently, multidrug-resistant bacteria have become a global health threat [2]. Therefore, there is an urgent need to find new effective agents to overcome drug resistance. In this regard, nanotechnology reveals new opportunities for the biosynthesis of nanoparticles with antibacterial properties to solve these challenges [3]. Nanoparticles are materials that show uniqueness in size (generally 1 to 100 nm), structure, physicochemical, electric, magnetic, thermal, mechanical, catalytic, optical scattering properties, and shape [4]. Green synthesis creates metallic nanoparticles through a bottom-up approach that includes a chemical reduction in which a natural product extract replaces a chemical-reducing agent [2]. Iron oxide nanoparticles (IONPs) are defined as "Nanozymes" due to their inherent enzyme-like activities and catalytic properties that are comparable to those of different oxidases such as peroxidases, catalase, sulfite oxidase, and superoxide dismutase [5]. Another feature

 doi:10.20944/preprints202310.0123.v1

of these particles is their potential to bind different biological molecules like peptides, enzymes, nucleic acids, lipids, fatty acids, and various metabolites. These nanoparticles have applications in optics, mechanics, biotechnology, engineering, remediation, microbiology, environmental medicine, and electronics, among others [6,7]. This review focuses on green methods for synthesizing iron oxide nanoparticles using bacteria, fungi, yeasts, plant extract, and organic waste. In addition, IONP's prospective antimicrobial applications are discussed in detail. This review will provide compelling information for researchers in the field of nanobiotechnology.

2. Green synthesis of iron oxide nanoparticles

2.1. Synthesis of iron oxide nanoparticles using microorganisms

The synthesis of iron oxide nanoparticles (IONPs) using microorganisms has several advantages over other methods due to the relative abundance of microorganisms, the generation of less toxic by-products for biomedical purposes, and lower cost [8]. Several microorganisms have the ability to accumulate and detoxify metals, and this property can be exploited to convert iron ions from metal salts into nanoparticles [9] using a variety of enzymes, cofactors, proteins, and secondary metabolites of the microorganism [9,10]. These molecules can act not only as reducing agents but also play an important role as stabilizers and protectors of nanoparticles [9]. Microbial proteins containing functional groups, such as hydroxyl, thiol, carboxylic acid, and amine, have been demonstrated to play a role in the stabilization of metal nanoparticles. These functional groups serve as binding sites for metal ions, which are subsequently reduced to form nanoparticles within the cell wall or the periplasmic space [11].

The synthesis of nanoparticles using microorganisms such as bacteria, fungi, yeasts, and algae can be carried out by intracellular or extracellular mechanisms [10]. The extracellular mechanism consists of the reduction of metal ions, such as iron, by proteins, enzymes, or components of the cell wall of microorganisms [12]. These components work as reducing agents and stabilizers and prevent the agglomeration of iron oxide nanoparticles [11]. For this type of synthesis, the microorganisms are grown under optimal conditions, the supernatant is collected by centrifugation and mixed with an aqueous solution of the metal salt, and the presence of nanoparticles is evidenced by the change in color of the medium [9]. Metal nanoparticles can also be formed when metal ions are trapped on the cell surface by electrostatic interaction and are reduced by enzyme action [11].

Intracellular mechanisms involve enzymatic reduction of metal oxide ions through electrostatic binding of metal ions to -COOH groups of the microbial cell wall, metal ions diffuse into the cell and interact with enzymes to form metal oxide nanoparticles [13, 14]. For this type of synthesis, the microorganisms are grown under optimal conditions, then the biomass is washed with sterile water and incubated with a solution of metal salts until a color change indicates the nanoparticle synthesis [9] (Figure 1).

Preprints (www.preprints.org) | NOT PEER-REVIEWED | Posted: 3 October 2023 doi:10.20944/preprints202310.0123.v1

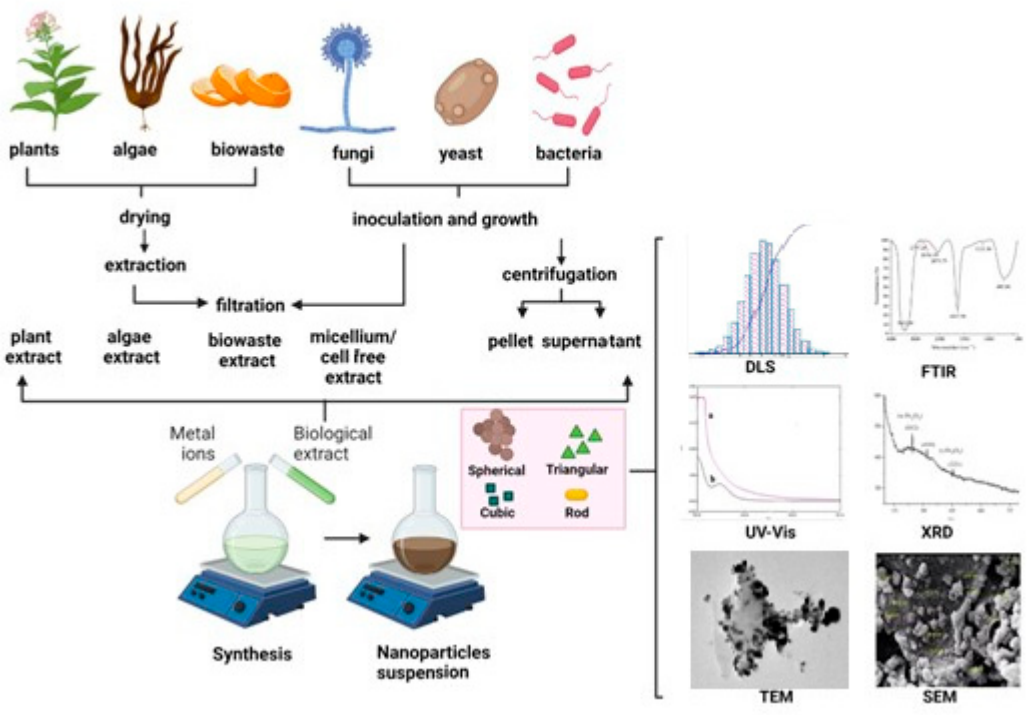

Figure 1. Schematic representation of green synthesis of iron oxide nanoparticles.

The reduction of metal ions is under the control of several factors, such as functional groups in the cell wall, type of strain, pH, temperature, culture medium, and metal salt concentration. These factors directly or indirectly affect the size, shape, composition, and performance of nanoparticles [15].

2.2. Synthesis of iron oxide nanoparticles using bacteria

The synthesis of iron oxide nanoparticles generally begins with the selection and isolation of bacteria, this includes culturing the strain on specific media such as BHI agar or nutrient agar, followed by incubation under controlled conditions at 35–37 °C for 24–48 h. Additionally, conditions such as carbon dioxide atmosphere may be required. The obtained individual colonies are transferred to the nutrient medium, such as Luria Bertani or nutrient broth, followed by incubation and centrifugation [16]. The supernatant (extracellular method) or the cell pellet (intracellular method) should be taken depending on the synthesis mechanism. The supernatant or sediment suspension is combined with the precursor salts, such as $FeCl_3.6H_2O$ or Fe_2O_3, in the desired volume and concentration. The reaction conditions are optimized by adjusting the pH to the preferred range (5–9), and the mixture is then incubated at different temperatures depending on the strain of bacteria used. After incubation, the color of the medium changes, for example, from dark red to dark brown, indicating the production of IONP's nanoparticles [17]. When using the intracellular approach, an additional step is required to remove the nanoparticles from inside the cell; for this, a heat shock must be performed by resuspending the cells in buffer, centrifuging, and then using liquid nitrogen followed by a steam bath at 37 °C. The supernatant is centrifuged and collected as a cytoplasmic extract [9,18]. Finally, the synthesized IONPs are dried and characterized. The synthesis of IONPs via different bacterial species is summarized in Table 1.

Preprints (www.preprints.org) | NOT PEER-REVIEWED | Posted: 3 October 2023 doi:10.20944/preprints202310.0123.v1

Table 1. Iron oxide nanoparticles synthesized by bacterial species.

Bacterial strain	Type of nanoparticle	Mechanism of synthesis	Size of nanoparticle (nm)	Nanoparticle morphology	Ref.
Alcaligens faecalis	Fe_2O_3	Extracellular	12.3	Irregular spherical	[19]
Actinobacter spp.	ɣ-Fe_2O_3	Extracellular	10–50	Crystal	[20]
Actinobacter spp.	FeO-NPs	Intracellular	10–40	Quasi-spherical	[21]
Bacillus cereus	Fe_3O_4	Extracellular	29.3	Spherical	[12]
Bacillus coagulans	FeO-NPs	Extracellular	-	-	[22]
Bacillus subtilis	Fe_3O_4	Extracellular	60–80	Spherical	[17]
Bacillus subtilis *Bacillus pasteurii* *Bacillus licheniformis*	Fe_3O_4	Extracellular	37–97	Rhombohedral	[23]
Desulfotomaculum acetoxidans	Fe_3O_4	-	21	-	[24]
Desulfovibrio, strain LS4	Fe_2O_3	Extracellular	19	Round shaped	[24]
Escherichia coli	Fe_3O_4	Extracellular	23 ± 1	Spherical	[25]
Geobacter sulfurreducens	Fe_3O_4	Extracellular	10–50	-	[26]
Gluconacetobacter xylinus	Fe_3O_4	Intracellular	50	-	[27]
Klebsiella oxytoca	Ferrihydrite nanoparticles	-	2–5	-	[28]
Lactobacillus casei	Fe_3O_4	Intracellular	10–15	Spherical	[18]
Lactobacillus fermentum	Fe_3O_4	Intracellular	10–15	Spherical	[16]
Leptothrix ochracea	-	Extracellular	100	Hollow tube	[29]
Magnetospirillum magneticum	Fe_3O_4	Intracellular	10–60	Cuboidal, rectangular, and spherical NPs	[30]
Magnetospirillum gryphiswaldense	Fe_3O_4	Extracellular/ Intracellular	25–55	Polydisperse	[31]
Microbacterium marinilacus	FeO-NPs	Extracellular	25–88	Irregular	[32]
Nitrospirae (MYR-1)	Fe_2O_3	Intracellular	40	Bullet-shaped	[33]
Pseudomonas stutzeri	Fe_2O_3	-	10-20	-	[34]
Paenibacillus polymyxa	FeO-NPs	-	26.65	Spherical	[35]
Proteus mirabilis	Fe_3O_4	Intracellular	1.44–1.92	Spherical	[36]
Pseudomonas	Fe_3O_4	Extracellular	23	Spherical	[25]

 doi:10.20944/preprints202310.0123.v1

aeruginosa					
Shewanella oneidensis	Fe_2O_3	Intracellular	30–43	Pseudo hexagonal shape	[37]
Streptococcus suis	Fe_3O_4	-	-	-	[38]
Thermoanaerobacter sp	Fe_3O_4	Extracellular	~13.0	Spherical	[39]
Thiobacillus thioparus	Fe_3O_4	Intracellular	-	-	[40]

2.3. Synthesis of iron oxide nanoparticles using fungi

The production of iron oxide nanoparticles via fungal synthesis is considered an attractive option due to its simplicity of scaling, the low cost of the materials necessary for growth, the capacity to produce high amounts of biomass even at an industrial scale, and the low toxicity of the residue [41,42]. In addition, fungal species have higher metal tolerance and bioaccumulation properties, facilitating the synthesis of metal nanoparticles [43]. Fungi are known to secrete large amounts of proteins, enzymes (i.e reductase enzymes [44]), and metabolites that can convert metal salts into various metal nanoparticles [13,45]. Researchers discovered that chitin, a key component of the fungal wall system, is involved in the formation of heavy metal complexes, which are linked to the synthesis of nanoparticles [46]. However, the mechanisms behind metal nanoparticle synthesis using fungi still need to be fully understood.

To optimize the synthesis, some factors must be considered, including the microorganism strain, growth parameters, sample preparation technique, metallic precursor, metallic salt concentration, pH, and reaction temperature [47]. Metal nanoparticles may be synthesized using fungi in a variety of ways, including employing fungal biomass, cell-free filtrate (CFF) from fungal culture, or fungal cell filtrate (FCF) [10]. The use of mycelium is one of the simplest approaches; this process involves culturing the selected fungus strain in an appropriate medium and then separating the mycelium by centrifugation. The mycelium is combined with a metal precursor salt solution and incubated for 4–5 days at 28 °C. The solution is then filtered to produce a colloidal suspension containing the synthesized nanoparticles [22,48]. Nanoparticles can also be synthesized using the cell-free filtrate, which is obtained by growing fungi in a suitable medium and separating the mycelium by filtration. After washing and resuspending the fungal biomass in distilled water, it is incubated on a rotary shaker for 1–5 days, and the filtrate is collected by separating the mycelium with filter paper. Finally, the cell-free filtrate is combined with a solution of iron precursor salts such as ferric chloride and incubated for a few hours on the rotary shaker to achieve IONPs synthesis [45]. For the IONPs synthesis method based on fungal cell filtrate (FFC), the fungal strain is cultivated in the appropriate medium, after which the culture medium is filtered, and the filtrate obtained is centrifuged and filtered again to obtain the final FFC. Finally, a $FeCl_3$ solution is stirred at room temperature for 5 min. An immediate visual change in color reveals IONPs synthesis [49].

On the other hand, relatively little is known about IONPs biosynthesis from yeast. This type of fungus has a widely varied metabolic and proteomic profile, which means it can produce a wide variety of compounds that have the potential to act as reducing agents [50]. However, more research is required to evaluate its potential and biosynthetic mechanism. Recent reports on the synthesis of IONPs by yeast and fungi are shown in Table 2.

Preprints (www.preprints.org) | NOT PEER-REVIEWED | Posted: 3 October 2023 doi:10.20944/preprints202310.0123.v1

Table 2. Synthesis of iron oxide nanoparticles using fungi and yeast.

Fungi	Location of synthesis	Type of nanoparticle	Size of nanoparticle (nm)	Nanoparticle morphology	Ref.
Alternaria alternate	Cell-free filtrate	γ-Fe_2O_3	75–650	Cubic	[51]
Aspergillus fumigatus	Fungal biomass	Fe_2O_3	42.4	Irregular spherical	[22]
Aspergillus japonicus	Fungal biomass	Fe_3O_4	60–70	Cubic	[48]
Aspergillus niger YESM 1	Fungal homogenate	Fe_3O_4	18-50	Spherical	[52]
Aspergillus niger BSC-1	Cell-free filtrate	Fe_3O_4	20–40	Orthorhombic	[41]
Aspergillus wentii	Fungal biomass	Fe_2O_3	46	-	[22]
Baker'syeast	Fungal biomass	Fe_2O_3	2–10	-	[53]
Candida bombicola	Fungal biomass	Fe_3O_4	8.5–4.5	-	[50]
Chaetomium globosum	Fungal biomass	Fe_2O_3	25.3	Irregular spherical	[22]
Cryptococcus humicola	-	Fe_3O_4	8-9	Spherical	[54]
Curvularia lunata	Fungal biomass	Fe_2O_3	20.8	Irregular spherical	[22]
Fusarium incarnatum	Fungal cell filtrate	Fe_3O_4	30.56 ± 8.68	Spherical	[49]
Fusarium oxysporum	Fungal biomass	Fe_3O_4	10-40	Cube	[42]
Neurospora crassa	Fungal biomass	Fe_3O_4	50	Coralline appearance	[55]
Phialemoniopsis ocularis	Fungal cell filtrate	Fe_3O_4	13.13 ± 4.32	Spherical	[49]
Pochonia chlamydosporium	Fungal biomass	Fe_2O_3	~12-50	Spherical	[22]
Thichoderma asperellum	Fungal cell filtrate	Fe_3O_4	25 ± 3.94	Spherical	[49]
Verticillium sp.	Fungal biomass	Fe_3O_4	100–400	Cubo-octahedrally	[42]

2.4. Synthesis of iron oxide nanoparticles using algae

Algae (microalgae and macroalgae) are commonly used to produce different metallic nanoparticles, and this has become an environmentally friendly option because it is a clean, non-toxic, and sustainable process with the potential to produce a wide variety of sizes, shapes, compositions, and physical and chemical properties [56]. Glycoproteins and different functional groups, such as carbonyl, hydroxyl, and carboxyl, as well as proteins, enzymes, alkaloids, carotenoids, vitamins, terpenes, and cell wall polysaccharides [57,58], are just a few of the biomolecules found in algae. Furthermore, algae can also accumulate heavy metals and produce secondary metabolites with anti-biological fouling effects [56,59]. These characteristics, together with the components they produce, are critical in the reduction, protection, manufacture, and stabilization of [10] nanoparticles [60]. For example, an aqueous extract of *Sargassum muticum* was used to synthesize cubic iron oxide nanoparticles from $FeCl_3$ at a temperature of 25 °C, and it was determined

Preprints (www.preprints.org) | NOT PEER-REVIEWED | Posted: 3 October 2023 doi:10.20944/preprints202310.0123.v1

that the polysaccharides in the algae extract were the main factor in the reduction of $FeCl_3$ to Fe_3O_4 nanoparticles with an average size of 18 ± 4 nm [58].

To synthesize nanoparticles from algae, the samples are washed with distilled water and then dried for 72 h under light [58]. The dried samples are then powdered, freeze-dried, weighed, and boiled by mixing the powder with the necessary volume of distilled water. To produce the extract, the boiled extract is subjected to a filtration step. The synthesis of the IONPs begins by combining the extract with a known amount of iron salts, such as $FeCl_3$ [58,61]. The color change in the media indicates that nanoparticle nucleation has occurred [56,62]. This process is facilitated by the biomolecules found in algae extract, which facilitate the aggregation and self-assembly of nucleonic particles. During this process, the most energetically favorable and stable particle shapes are generated, with cubes, hexagons, pentagons, bars, spheres, triangles, and wires being the most prevalent [63]. Table 3 summarizes information on nanoparticles obtained from various algae extracts.

Table 3. Synthesis of iron oxide nanoparticles using algae.

Algae	Location of synthesis	Type of nanoparticle	Size of nanoparticle (nm)	Nanoparticle morphology	Ref.
Chaetomorpha antennina	Cell-free extract	Fe_3O_4	9–10	-	[64]
Chlorella K01	Dried powder	Fe_3O_4	76.5	Spherical	[65]
Colpomenia sinuosa	Dried powder	Fe_3O_4	11.24–33.71	Spherical	[61]
Colpomenia sinuosa	Dried powder	Fe_3O_4	17.78	Cubic	[66]
Kappaphycus alvarezzi	Dried powder	Fe_3O_4	14.7	Spherical	[67,68]
Padina pavonica	Dried powder	Fe_3O_4	31.41	Spherical	[66]
Padina pavonica	Freeze-dried powder	Fe_3O_4	10–19.5	Spherical	[69]
Petalonia fascia	Dried powder	Fe_3O_4	9.42,	Spherical	[66]
Pterocladia capillacea	Dried powder	Fe_3O_4	16.85–22.47	Spherical	[61]
Sargassum acinarium	Freeze-dried powder	Fe_3O_4	21.6–27.4	Spherical	[69]
Sargassum muticum	Freeze-dried powder	Fe_3O_4	18	Cubic	[58]
Spirulina platensis	Dried powder	Fe_3O_4	10	-	[70]
Turbinaria turbinata	Cell-free extract	Fe_3O_4	8–14	-	[64]

2.5. Synthesis of iron oxide nanoparticles using plants

Because microorganism-based synthesis requires long incubation periods, extensive research has been conducted on plant-based synthesis of iron oxide nanoparticles since plants, on the other hand, reduce metal salts in a shorter time [9]. Plant extracts used for the biosynthesis of nanoparticles can be obtained from the leaves, flowers, bark, roots, fruits, and stems [10]. Bioactive compounds of these extracts, including mainly tannins, phenols, alkaloids, saponins, organic acids, flavonoids, and vitamins, work as reducing agents for metal salts and stabilizers of nanoparticles [10,71].

Depending on the iron precursor used to form the Fe^0 metal, electron-rich biomolecules containing hydroxyl groups (-OH) have the ability to effectively reduce iron ions from the divalent

Preprints (www.preprints.org) | NOT PEER-REVIEWED | Posted: 3 October 2023 doi:10.20944/preprints202310.0123.v1

or trivalent oxidation state (Fe^{2+} or Fe^{3+}) [72,73]. The characteristics of the synthesized nanoparticles are mostly determined by discrete parameters such as plant extract type, volume ratio of the extract, metal salt solutions, and reaction variables such as pH, temperature, and incubation time [72,74].

To obtain the plant extract, the first step is to collect the desired part of the plant of interest, which is then washed with distilled water to remove any contaminants, dried at room temperature, and then ground into a fine powder to provide a good surface for extraction [73]. The active compounds of this powder are extracted by mixing it with the appropriate solvent, either hot or cold; the most frequently employed solvents are water, methanol, ethanol, or aqueous dilutions of these [75,76]. Finally, it is filtered, and the clear solution is mixed with the iron precursor salts (iron chloride, iron nitrate, or iron sulfate) to produce IONPs. In this case, the chemical components in the extract also stabilize the nanoparticles, and the change in color of the solution, which depends on the kind of salt used, intensifies as the nanoparticles are synthesized [7,73,77]. As shown in Table 4, various parts of plants have been studied for the environmentally safe synthesis of iron oxide nanoparticles.

Table 4. Synthesis of iron oxide nanoparticles using plants.

Plant species	Part of the plant	Type of nanoparticle	Size of nanoparticle (nm)	Nanoparticle morphology	Ref.
Medicago sativa	Leaves	Fe_2O_3/Fe_3O_4	3.1	Spherical	[78]
Aloe barbadensis	Leaves	Fe_2O_3	80–100	Spherical	[79]
Amla	Seeds	Fe_2O_3	2-5	Spherical	[140]
Arisaema amurense	Root	Fe_2O_3	24.55 ± 6.9	Nearly spherical	[80]
Artemisia annua	Leaves	Fe_2O_3/Fe_3O_4	4.7 ± 0.8	Spherical	[81]
Avecinnia marina	Flowers	FeO-NPs	10–40	Non-uniform	[82]
Azadirachta indica	Leaves	Fe_3O_4	9-12	Irregular	[83]
Calliandra haematocephala	Leaves	Fe_3O_4	85.4–87.9	Bead-like spherical	[84]
Carica papaya	Leaves	α-Fe_2O_3	2.15	Spherical to agglomerate	[6]
Coriandrum sativum	Leaves	FeO-NPs	20–90	Spherical	[85]
Colocasia esculenta	Leaves	FeO-NPs	15	Spherical	[86]
Cynometra ramiflora	Leaves	FeO-NPs	-	Agglomerated	[87]
Cynara cardunculus	Leaves	Fe_3O_4	13.5	Semi-spherical	[88]
Daphne mezereum	Leaves	Fe_3O_4	6.5–14.9	Spherical	[89]
Eichhornia crassipes	Leaves	FeO-NPs	>100	Rod-shaped	[90]
Eucalyptus globulus	Leaves	β-Fe_2O_3	100	Spherical	[91]
Eucalyptus globulus	Leaves	Fe_3O_4	2.34 ± 0.53	Spherical	[92]
Euphorbia wallichii	Leaves	FeO-NPs	10–15	Spherical	[93]

Preprints (www.preprints.org) | NOT PEER-REVIEWED | Posted: 3 October 2023 doi:10.20944/preprints202310.0123.v1

Euphorbia herita	Leaves	Fe_3O_4	25–80	Spherical	[94]
Gardenia resinifera	Leaves	α-Fe_2O_3	3–8	Spherical	[95]
Grapes	Seeds	Fe_3O_4	35	Spherical	[96]
Green tea	Leaves	FeO-NPs	5.7 ± 4.1	Spherical	[97]
Hibiscus rosasinensis	Flower	FeO-NPs	65	Spinel	[98]
Sageretia thea	Leaves	Fe_2O_3	29	Tetragonal crystalline	[99]
Lagenaria siceraria	Leaves	Fe_3O_4	30–100	Cube	[100]
Lantana camara	Leaves	FeO-NPs	-	Crystalline nanorods	[101]
Laurus nobilis L	Leaves	α-Fe_2O_3	8.03 ± 8.99	Spherical	[3]
Lawsonia inermis	Plant	FeO-NPs	150–200	Spherical	[102]
Mangifera indica L	Leaves	FeO-NPs	-	Polycrystalline nanorod	[103]
Mansoa alliacea	Leaves	β-Fe_2O_3	18.22	Spherical nanoparticles	[77]
Moringa oleifera	Leaves	FeO-NPs	15.01 ± 6.03	Rods	[1]
Plantago major	Leaves	FeO-NPs	4.6–30.6	Spherical	[104]
Platanus orientalis	Leaves	α-Fe_2O_3 and γ-Fe_2O_3	38	Spherical	[105]
Psidium guajava	Leaves	FeO-NPs	1–5	Spherical	[106]
Punica granatum	Seeds	Fe_2O_3	25–55	Semi spherical	[71]
Rheum emodi	Roots	α-Fe_2O_3	12	Spherical	[139]
Ruellia tuberose	Leaves	FeO-NPs	20–80	Hexagonal rods	[107]
Rumex acetosa	Plant	FeO-NPs	40	Amorphous	[74]
Sesbania grandiflora	Leaves	FeO-NPs	25–60	Agglomerated non-spherical	[108]
Soya bean	Sprouts	Fe_3O_4	8	Spherical	[109]
Tamarix aphylla	Leaves	Fe_2O_3	5–100	Oval	[110]
Terminalia belerica	Fruits	FeO-NPs	15–23	Spherical	[111]
Tridax procumbens	Leaves	Fe_3O_4	80–100	Irregular spherical	[112]
Vaccinium corymbosum	Leaves	FeO-NPs	52.4	Irregular shape non agglomerated	[113]

2.6. Green synthesis of iron oxide nanoparticles using from biological waste products

Agro-wastes are abundantly produced during the processing of agricultural products and are frequently discarded into the environment, causing pollution [114]. Agro-waste has been found to be rich in biomolecules such as flavonoids, phenolics, and proteins that can serve as bioreductant agents in the green synthesis of diverse metallic nanoparticles [115]. A new effort to expand the use of agro-wastes as sources of biomolecules in green nanotechnology have received considerable attention, and various agro-wastes have been documented for their relevance in nanobiotechnology [115]. As a result, a range of metallic nanoparticles have been successfully synthesized from agro-industrial wastes, and extracts from these residues have been employed as reducing and stabilizing agents in

Preprints (www.preprints.org) | NOT PEER-REVIEWED | Posted: 3 October 2023 doi:10.20944/preprints202310.0123.v1

the majority of cases [116]. The nanoparticles produced in this way have a wide range of activities, including antimicrobial, antioxidant, anticorrosive, and cytotoxic against cancer cells, among others [116–119]. In general, extracts containing active biomolecules that promote the formation of nanoparticles can be prepared using a simple hot water extraction process of dried and ground agro-waste materials [115]. Information on the nanoparticles obtained from biological waste is highlighted in Table 5.

Table 5. Iron oxide nanoparticles synthesized by biological waste.

Biological source	Type of waste	Size of nanoparticle (nm)	Nanoparticle morphology	Ref.
Ananas comosus	Fruit peel	10–16	Spherical	[117]
Acacia mearnsii	Biochar	18–35	-	[120]
Camellia sinensis	Tea waste	28.5	Spherical	[118]
Citrus Aurantifolia	Fruit peel	3–10	-	[119]
Cocos nucifera L	Fruit peel	10–100	Clustered	[121]
Coffee	Waste hydrochar	10–40	Spherical	[122]
Cynometra ramiflora	Fruit peel	10–25	Agglomerated	[123]
Juglans regia	Dried green husk	12.6	Cubic	[124]
Lemon	Fruit peel	3 and 10	Orthorhombic	[119]
Malus domestica *Citrus limon*	Fruit peel	17–25	Spherical	[125]
Orange	Fruit peel	50	Quasi spherical	[116]
Plantain	Fruit peel	30–50	Spherical	[126]
Punica Granatum	Fruit peel	40	Rod shaped	[127]
Rambutan	Fruit peel	100–200	Agglomerated spinel	[128]
Rice	Straw	9.9 ± 2.4	Aggregated spherical	[129]
Tangerine	Fruit peel	50	Spherical	[130]
Watermelon	Rinds	2–20	Spherical	[131]

3. Characterization methods

The green synthesis methods of metallic nanoparticles are continually being improved and optimized to achieve comparable results (size and morphology) to physical and chemical methods. Usually, a change in the color of the reaction mixture indicates the formation of nanoparticles; however, this does not guarantee their formation, so additional processes must be used to identify the particles formed. Continuous UV spectra of the reaction mixture are one of the most frequently applied methods to confirm the formation of nanoparticles [92,132,133] Currently, a variety of characterization methods are useful for evaluating the properties and uses of synthesized nanoparticles, as well as optimizing synthesis procedures [134]. However, no single instrument can characterize all material properties. As a result, numerous complementary and confirmatory techniques for nanoparticle characterization should be applied (Table 6).

Table 6. Characterization techniques for nanoparticles.

Property	Characterization techniques
Size	TEM, XRD, DLS, NTA, SAXS, HRTEM, SEM, AFM, EXAFS, FMR, DCS, ICP-MS, UV-Vis, MALDI, NMR, TRPS, EPLS, magnetic susceptibility

 doi:10.20944/preprints202310.0123.v1

Shape	TEM, HRTEM, SEM, AFM, STEM, EPLS, FMR, 3D-tomography
Chemical composition	XRD, XPS, ICP-MS, ICP-OES, SEM-EDX, NMR, MFM, LEIS, EELS
Crystal structure	XRD, EXAFS, HRTEM, electron diffraction, STEM
Surface Charge	Zeta potential, EPM
Magnetic properties	SQUID, VSM, Mössbauer, MFM, FMR, XMCD, magnetic susceptibility

The most common nanoparticle parameters studied include size, shape, charge, and surface topology [134]. However, characterizing nanoparticles remains difficult due to the sample preparation procedure, and the characterization technique utilized is directly dependent on the properties required [135].

One of the most important parameters to evaluate is particle size and size distribution, which correlates to the particle's external dimensions. Because this property can determine other properties and the behavior of the final product [136,137], it is important for biological and biomedical applications. This property frequently differs depending on the method employed to evaluate it, which can be attributable to a variety of factors. For example, different methods evaluate different aspects of nanoparticle dimensions, or the method can induce a change in the effective particle size [138]. Among the most common methods for determining the size of iron oxide nanoparticles are: Transmission Electron Microscopy (TEM) [119,139–141], Scanning Electron Microscopes (SEM) [71,119,142,143], X-ray Diffraction (XRD) [142,144–146], Dynamic Light Scattering (DLS) [147–149], High-resolution Transmission Electron Microscopy (HRTEM) [150–152], Scanning Transmission Electron Microscopy (STEM) [92].

The physical appearance of a particle (morphology), which comprises shape and surface topography, is important to the behavior of iron oxide nanoparticles. Morphology affects different properties like dispersion, functionality, and toxicity. This property, like the size, is evaluated through direct viewing of the particles, so commonly, electron microscopy techniques are utilized. Among the various forms of iron oxide nanoparticles that have been reported are: round (SEM) [153], spherical (SEM) [142,143], (STEM) [92], (TEM) [146], spheroidal (HRTEM) [152], cubic (SEM) [143], rectangular and triangular (HRTEM) [151], rhombohedral [119], and needle-like (FESEM and HRTEM) [154].

Another important property to determine is the chemical composition of iron oxide nanoparticles. It can be characterized both in terms of surface and bulk chemistry and can be measured at the ensemble or single nanoparticle level. It is mostly determined using spectroscopic techniques, which may be paired with microscopy to attain single-particle level resolution, with the most often used methods being XRD [140,152,155,156], EDS [92,155,157] and EDX [144,158–160]. Because the nanoparticle's external layer interacts with the surrounding environment, determining its composition (surface chemistry) is also important and can be obtained using different techniques like Auger electron spectroscopy [161,162], X-ray photoelectron spectroscopy [163–165], or inductively coupled plasma mass spectrometry [166].

Along with the chemical composition, another property of importance in the study of IONPs is the crystalline structure of the nanoparticles. In general, XRD is used to determine the three-dimensional arrangement of the atoms in nanoparticles as well as the different phases. However, it has been found that nanoparticles smaller than 5 nm have an impact on the XRD-observed patterns [167]. SAED [168], which is being used increasingly commonly, is a method for a more accurate representation of the crystalline structure of iron oxide nanoparticles [146,149,155].

The charge of nanoparticles in suspension is also an important property to consider. The surface charge is the charge formed on the surface of the nanoparticle as a result of proton adsorption or desorption at hydroxylated sites, and due to the difficulties of directly measuring this charge, the particle's zeta potential is frequently determined. The zeta potential is the difference in potential between the stationary layer of the dispersion medium attached to the dispersed particle and the

 doi:10.20944/preprints202310.0123.v1

mobile dispersion medium [168] and can be measured by titration [169] or electrophoresis [92,170,171]. It is important because it is used as an indicator of colloidal stability, which is a critical parameter for many emulsions or dispersions; additionally, it has been used to investigate the interaction of iron oxide nanoparticles with various biological systems, including human cells [172], bacteria [173], and proteins [174].

Nanoparticles' magnetic behavior differs from that of bulk materials, as do other properties. Furthermore, the synthesis method, size, and shape of IONPs all affect the magnetic properties of the nanoparticles. When the particle size is between nano and micro, it exhibits superparamagnetism, resulting in low remanent magnetization and a coercive field. As a result, the nanoparticles can interact with an external magnetic field, but in the absence of this field, the particles exhibit no magnetism. Because of this property, superparamagnetic iron oxide nanoparticles (SPIONs) have a high potential for use in biomedical applications, including controlled drug delivery, chemotherapy, drug formulations, hyperthermia treatment, and radioimmunotherapy, among others [136]. Magnetometry techniques such as VSM (vibrating sample magnetometer) [80,148,158] and SQUID (superconducting quantum interference device) magnetometry [175] are used to determine the net magnetization of nanoparticles.

3.1. UV–VIS spectroscopy

UV–vis spectroscopy, which is based on the Beer-Lambert law, is a common method for investigating the optical and structural properties of nanomaterials, such as shape, size, agglomeration state, concentration, refractive index, and colloidal stability [176–180]. This technique, as previously stated, can be used to confirm the formation of IONPs. Due to their surface plasmon resonance (the resonance of the metal's conduction electrons), metal nanoparticles with a diameter of less than 100 nm efficiently scatter optical light, however, as the particle size increases, the absorption spectra can change, shifting toward longer wavelengths. The nanoparticle's composition, environment, form, and size affect the plasmon resonance's bandwidth, magnitude, and wavelength peak [181]. Greenly synthesized iron oxide nanoparticles typically have absorption spectra with peaks in the 290–370 nm region and an estimated energy band gap from 2.9 to 4.22 eV [82,182–184].

3.2. TEM and HRTEM

Transmission electron microscopy (TEM) is a characterization technique used to study the dynamics of physical and chemical processes of the nanostructure at an atomic resolution [185]. An electron beam interacts with the sample, and the transmitted electrons are used to form the image by magnifying and focusing them using an objective lens. The interaction of the electron beam with the sample in the TEM image results in diffraction processes as opposed to absorption processes, which occur in the light microscopic image. Because the sample will be exposed to a high vacuum during the analysis, it must be prepared to endure both the electron beam and the high vacuum chamber [186]. The difference in electron densities of the structures, the density and thickness of the sample, the objective aperture´s diameter, and the energy of the electrons all influence TEM images [187]. Additionally, the contrast image can be generated using either unscattered electrons (light field image) or deflected electrons (dark field image). This technique is widely used to characterize the morphology of nanostructures, such as particle size [188,189], agglomeration state [107], electronic state, and chemical composition [190]. Furthermore, depending on the sample, the electron energies for the beam are generally 100 keV for conventional images and 1 MeV for high-resolution imaging [186]. High-resolution transmission electron microscopy (HRTEM) is a TEM imaging mode that provides atomic-level imaging of a nanoparticle's crystalline structure. With this level of detail, it is feasible to image crystal structures, crystal defects, and individual atoms [181].

3.3. SEM

Scanning Electron Microscopy (SEM) is a non-destructive analytical method used for surface and microstructural analysis that also uses an electron beam, typically ranging from 1 to 30 keV, that

Preprints (www.preprints.org) | NOT PEER-REVIEWED | Posted: 3 October 2023 doi:10.20944/preprints202310.0123.v1

scans the surface of the sample. [186,191]. This technique is also useful for determining the purity, homogeneity, and degree of dispersion [192]. When the electron beam strikes a nanoparticle, it emits X-rays as well as three types of electrons: backscattered (or primary) electrons, secondary electrons, and Auger electrons. SEM makes use of both primary and secondary electrons, with the latter being used to generate high-resolution images that reveal features as small as 1-5 nm [192]. An advantage of SEM characterization is that it also helps to study the surface characteristics of the sample of IONPs, given the three-dimensional appearance of the surface structure [100].

Nanoparticles do not require pretreatment since metals conduct electricity when struck by an electron beam, whereas non-metallic materials do. To do this, they are often coated with gold to create a thin coating of conductive material. In standard SEM, however, water molecules evaporate in a vacuum, producing an impediment for the electron beams and obscuring image clarity; hence water removal is important.

3.4. EDX

Energy-dispersive X-ray spectroscopy (EDX) is a technique for determining the purity and elemental composition of synthesized nanoparticles [193]. As previously stated, when an electron beam hits a nanoparticle, X-rays are released along with the three types of electrons, and the energy of the generated X-rays depends on the material under investigation, hence EDX is a technique used in combination with SEM. An image of each element in the sample may be obtained by moving the electron beam over the material, giving an overall mapping of the sample by examining near and at the surface elements and estimating its proportion at different points [181].

3.5. XRD

X-ray diffraction (XRD) is a non-destructive technique used to analyze the crystallographic structure of a material. It can also be used to determine element proportions, the position of atoms in the unit cell, unit cell characteristics, and the number of atoms in the unit cell [194]. The interaction of the X-ray beam with the atomic planes results in partial beam transmission, with the remainder absorbed, refracted, scattered, and diffracted by the sample [181]. High-resolution powder X-ray diffraction (HRXRD) can be used to obtain finer information about the structure of nanoparticles, such as ion spacing and bond length of related substances in single crystal cells, and it is one of the most widely used techniques for determining crystalline perfection and defect studies in single crystals [195], as well as detailed studies of structure and phase transformation in materials [196].

The lattice and structural characteristics may be determined by measuring the diffraction angle obtained when an X-ray beam is incident on the nanoparticles. For example, the crystal size may be determined by applying the original Scherrer equation or a modified version (1).

$$L = k/\beta\cos\theta \quad \text{or} \quad \ln\beta = \ln k/L + \ln 1/\cos\theta \tag{1}$$

Where L = average crystallite size, k = constant related to shape (0.94), λ = wavelength of X-ray, β = peak width of the diffraction peak profile at half maximum height, and θ = Bragg's angle [197].

3.6. DLS

Dynamic light scattering (DLS), also known as photon correlation spectroscopy or quasi-elastic light scattering, is a frequently employed technique for determining the size distribution profile of NPs in colloidal solutions in the nano- and submicrometer ranges [134]. When a monochromatic laser beam strikes a suspension of tiny particles, the light scatters in all directions, depending on the size and shape of the nanoparticles [198]. Given that the nanoparticles in suspension are in continuous motion due to Brownian motion, the scattering intensity changes over time and offers information on particle size, allowing the hydrodynamic diameter of NPs in solution to be determined. The hydrodynamic diameter is the diameter of the NPs and solvent molecules that diffuse at the same rate as the colloid [199,200]. DLS can also measure the stability of nanoparticles over time, which is useful for understanding how they could behave in different environments and applications [201].

 doi:10.20944/preprints202310.0123.v1

4. Antimicrobial properties of green-mediated synthesis iron oxide nanoparticles

4.1. Antibacterial activity.

Considering the emergence of antibiotic-resistant strains as the leading public health threat worldwide, the search for novel molecules with antibacterial potential is of particular interest. Free iron ions and various metal and metal oxide NPs like silver, ZnO, Al_2O_3, and TiO_2 have been screened as bactericidal or antibacterial agents [202]. However, the main concern when using nanoparticles with antibacterial properties is their high toxicity, which has been reported for ZnO [63, 64]; thus, a nanoparticle that is biologically active against bacteria and biocompatible is needed [61,62]. In this context, IONPs have recently emerged as an alternative due to their bactericide properties and biocompatibility *in vivo* and *in vitro*. Despite the potential of nanoparticles as antimicrobial agents, some risks have been reported concerning human health and the environment. In contrast to this, IONPs have been shown to be safe and do not cause toxicity in mammalian cell cultures [203,204], a highly desired characteristic to use in biomedical, clinical, and pharmaceutical applications. The most relevant IONPs with biological activity are Fe_2O_3, magnetite Fe_3O_4, and limonite $Fe_2O_3*H_2O$ [205].

4.1.1. Mechanisms of Antibacterial IONPs Activity.

The primary mechanism by which metal oxide nanoparticles exhibit bactericidal activity is through the regeneration of reactive oxygen species (ROS) [206,207]. ROS species, such a as superoxide radicals (O_2^-), hydroxyl radicals (OH^-), hydrogen peroxide (H_2O_2), and singlet oxygen ($^1O_2$) are involved in this process. It has been proposed that the combined interaction between IONPs and ROS species might be responsible for the bactericidal activity [208]. Furthermore, the interaction of Fe^{2+} ions and ROS species leads to the formation of free hydroxyl radicals and hydrogen peroxide, ultimately resulting in bacterial death. Various mechanisms of bactericidal action, which have recently been reported, are described below [209].

4.1.2. Membrane disruption

As mentioned, iron oxide nanoparticles can interact with bacterial cell membranes via electrostatic interactions, producing harmful oxidative stress in the bacterium by generating free radicals [210]. Additionally, intracellular oxygen in aerobic bacteria oxidizes zero-valent iron, causing irreversible oxidative damage to the cell. Moreover, because of their small size, IONPs can enter the cell and cause physical damage to the cell wall, limiting cellular growth, replication, and even communication [206].

In *E. coli*, electron microscope analysis revealed that Fe_2O_3 nanoparticles bind to the cell wall and even penetrate into the cytoplasm, where they accumulate, causing vacuole formation and cell wall disruption [211,212]. Fe_3O_4 nanoparticles bind to the formate hydrogenlyase complex (FHL) found in Gram-negative bacteria cell walls, generating a gradient in the inner membrane that has a strong antimicrobial effect on these bacteria [213]. Another mechanism that causes membrane disruption is disturbing the activity of F0/F1-ATPase, which reduces the membrane redox potential and, as a result, the H^+ rate [213]. The size and shape of IONPs have been suggested as key factors in elucidating their bactericidal activity [214].

4.1.3. Protein and DNA damage

ROS damage DNA molecules through their genotoxic action [215]. A decrease in the activity of antioxidant system enzymes (SOD, catalase, and glutathione reductase) might cause an increase in ROS concentration [67]. Metal ions are able to bind the mercapto (-SH), amino (–NH), and carboxyl (–COOH) groups of proteins, including enzymes, causing inactivation or partial inhibition [214]. IONPs can reduce the expression of antibiotic-resistance genes (ARGs) in antibiotic-resistant bacteria found in operating rooms [205]. The capacity of nanoparticles with small sizes to inhibit DNA replication by inactivating topoisomerase has also been reported [216]. ROS interacts with thiol

Preprints (www.preprints.org) | NOT PEER-REVIEWED | Posted: 3 October 2023 doi:10.20944/preprints202310.0123.v1

groups in membrane proteins, generating oxidative stress, which denatures the protein, resulting in membrane impermeability and, finally, microbial death [22].

4.1.4. Antibiofilm activities

The physicochemical properties of nanoparticles, such as surface charge and hydrophobicity, are important when evaluating their antibiofilm activity because they influence their capacity to adsorb and penetrate biofilms [217,218]. Positively charged and neutral Fe_3O_4 nanoparticles have been shown to reduce biofilm formation in *Streptococcus mutans*, the primary cause of caries, as compared to negatively charged IONPs [219]. It has also been observed that IONPs decreases alginate production, which is a key component of the exopolysaccharide of *P. aeruginosa* biofilm. This reduction is dose-dependent at concentrations ranging from 0.8 to 64 μg/mL [220]. Superparamagnetic iron oxide nanoparticles (SPIONs) cause cell death and biofilm destruction due to vibration damage, local hyperthermia, and ROS generation [221]. These factors lead to the dissociation of bacteria from a biofilm, damage to the bacterial cell wall, membrane rupture, the fusion of different cells with each other, and death [222].

A list of relevant bacteria in the medical field that are susceptible to IONPs is presented in Table 7.

Table 7. Antibacterial properties of IONPs from natural sources.

Treated Bacterial Strain	Biological source for IONP generation	Antibacterial assay	Size of nanoparticle (nm)	Nanoparticle morphology	Ref.
Escherichia coli	*Moringa M. oleifera*	WDM	15.01 ± 6.03	Rod-like morphology	[1]
	composite of Psidium guavaja-Moringa oleifera	WDM	82 ± 7.0	Spherical	[223]
	Zea mays L.) ear leaves	WDM	37.86	Spherical	[224]
	Xanthomonas campestris	WDM	20–80	Polymorphous, spherical, oval and hexagonal.	[225]
	Penicillium sp.	DDM	11.3	Spherical	[45]
	Penicillium brevicompactum	DDM	30–50	Spherical	[226]
	Glycosmis mauritiana; Rutaceae/Leaves	DDM	≤100	Spherical	[133]
	Couroupita guianensis,Lecythidaceae/fruit extract	DDM	17	Spherical	[227]
	Nigella sativa seed extract	DDM	31.45	Spherical	[228]
	Piper betel leaves extract	WDM	25.17	Cubic	[229]
Klebsiella pneumoniae	*Penicillium sp.*	DDM	11.6	Spherical	[45]
	Zea mays L.) ear leaves	WDM	37.86	Spherical	[224]
	Agrewia optiva (Dhaman or Biul) and Prunus persica (Peach) leaf extract	WDM	15–60 (AO) 13–70 (PP)	Spherical, granular	[230]
	Papaver somniferum	WDM	38 ± 13	Elliptical or Spherical	[231]
	Glycosmis mauritiana; Rutaceae/Leaves	DDM	≤100 nm	Spherical	[133]
	Couroupita guianensis,Lecythidaceae/fruit extract	DDM	17	Spherical	[227]

Preprints (www.preprints.org) | NOT PEER-REVIEWED | Posted: 3 October 2023 doi:10.20944/preprints202310.0123.v1

Pseudomona aeuruginosa	*Penicillium sp.*	DDM	11.6	Spherical	[45]
	Moringa M. oleifera	WDM	15.01 ± 6.03	Rod-like morphology	[230]
	Agrewia optiva (Dhaman or Biul) and Prunus persica (Peach) leaf extract	WDM	15-60 (AO) 13-70 (PP)	Spherical, granular	[230]
	Papaver somniferum	WDM	38 ± 13	Elliptical or Spherical	[231]
	Withania coagulans/Berries	DDM	15–20	Nanorods	[232]
	Aloe vera/leaf extract	cellular damage assessed by SEM	8.26	Cubical, Rhomboidal, Spherical	[233]
Salmonella sp	*Acorus calamus/rhizome*	WDM	20–30	Spherical	[234]
	Piper betel leaves extract	WDM	25.17	Cubic	[228]
	composite of Psidium guavaja-Moringa oleifera	WDM	82 ± 7.0	Spherical	[223]
	Moringa M. oleifera	WDM	15.01 ± 6.03	Rod-like morphology	[230]
Staphylococcus aureus	*Penicillium sp.*	DDM	12	Spherical	[45]
	Composite of Psidium guavaja-Moringa oleifera	WDM	82 ± 7.0	Spherical	[106]
	Moringa M. oleifera	WDM	15.01 ± 6.03	Rod-like morphology	[106]
	Agrewia optiva (Dhaman or Biul) and Prunus persica (Peach) leaf extract	WDM	15–60 (AO) 13–70 (PP)	Spherical, granular	[230]
	Penicillium brevicompactum	DDM	30–50	Spherical	[226]
	Glycosmis mauritiana; Rutaceae/Leaves	WDM	≤100	Spherical	[133]
	Withania coagulans/Berries	WDM	15–20	Nanorods	[232]
	Couroupita guianensis, Lecythidaceae/fruit extract	WDM	17	Spherical	[227]
	Nigella sativa seed extract	WDM	31.45	Spherical	[229]
	Piper betel leaves extract	WDM	25.17	Cubic	[228]
Streptococcus pyogenes	*Zea mays L.) ear leaves*	WDM	37.86	Spherical	[224]
	Agrewia optiva (Dhaman or Biul) and Prunus persica (Peach) leaf extract	WDM	15–60 (AO) 13–70 (PP)	Spherical	[230]
	Piper betel leaves extract	WDM	25.17	Cubic	[228]

WDM: Well diffusion method. DDM: Disk diffusion method.

4.2. Antifungal activity

Iron oxide nanoparticles are a promising and safe antifungal agent with many applications, including medicinal, agricultural, and environmental applications [235]. Due to the benefits of sustainability, environmental considerations, and less toxic waste production, green synthesis of nanoparticles used for biomedical applications is gaining popularity over chemically synthesized

Preprints (www.preprints.org) | NOT PEER-REVIEWED | Posted: 3 October 2023 doi:10.20944/preprints202310.0123.v1

agents. Research on the antifungal activity of IONPs derived from green synthesis is still limited, although results against a wide range of pathogenic fungi are promising [236] (see also Table 8).

For instance, IONPs (mixed Fe_2O_3 and Fe_3O_4) synthesized using tannic acid in a green method showed antimycotic activity against T*richothecium roseum, Cladosporium herbarum, Penicillium chrysogenum, Alternaria alternata*, and *Aspergillus niger [236].* The antifungal activity was measured by inhibiting spore germination and determining the zone of inhibition (agar well diffusion assay) of fungal pathogens using a concentration of 0.5 mg/ml in both assays, with an inhibition range of 87.74% – 70.67% and an inhibition zone ranging from 28.67 mm – 18.00 mm, respectively (Table 8). The minimum inhibitory concentration (MIC) varied between 0.063 mg/mL and 0.016 mg/mL for the most sensitive pathogens, *Penicillium chrysogenum*, and *Aspergillus niger*, and was comparable with the MIC value shown by the conventional fungicide hexaconazole, which was used as a standard control [236].

Mixed α-Fe_2O_3 and γ-Fe_2O_3 IONPs synthesized from $Fe(NO_3)_3{\cdot}9H_2O$, using *Platanus orientalis* leaf extract in an aqueous phase green synthesis approach also showed promising antifungal activity against *Aspergillus niger* and even stronger activity against *Mucor piriformis*, with inhibition zones in the agar well diffusion assay of 16 mm and 26 mm, respectively, using 75 µL of 0.10 mg/mL NPs. These inhibition zones were also equivalent to hexaconazole (Table 8) [105]. The authors attributed the high activity against *Mucor piriformi* to the fungus's stronger surface interaction with the IONPs.

IONPs generated from $FeCl_3.6H_2O$ with green and black tea leaf extracts were tested against *Aspergillus flavus* and *Aspergillus parasiticus* strains and compared with the antifungal activity of copper and silver nanoparticles. Furthermore, their effects on aflatoxin production and adsorption were also evaluated. While silver nanoparticles had greater antimicrobial activity, IONPs displayed the highest adsorption capabilities of aflatoxin B_1, giving them an advantage in applications such as food safety. A concentration of 100 µg/mL IONPs reduced the aflatoxin production by 39.2 – 43.5% in *Aspergillus flavus* and 47.1 – 51.6% in *Aspergillus parasiticus*, suggesting significant inhibition of the fungal pathogens (Table 8) [237].

Several other studies have been performed using a variety of biological source materials and green synthesis approaches for IONPs and tested against various fungal strains, which are summarized in Table 8. Briefly, *Laurus nobilis* L. extracts for IONPs generation results in antifungal activity against *Aspergillus flavus* and *Penicillium spinulosum* [3]; leaf extract of *Euphorbia helioscopia* aids IONPs generation with inhibitory activity against *Cladosporium herbarum [238]*; and *Euphorbia hirta* leaf extract can be used to generate IONPs with antifungal activity against *Aspergillus fumigatus, Aspergillus niger and Arthogrophis cuboida* (Table 8) [94].

It is worth noting that nanoparticles generally allow for surface modification to either change the physicochemical properties or even for targeted drug or bio-cargo delivery via coating/adsorption/binding of therapeutic and bioactive molecules. One such example is chitosan-coated IONPs with antimycotic activity against *Fusarium solani, Aspergillus niger*, and *Candida albicans* [239]. While these IONPs were not synthesized in a green approach, the same method used for their modification should be applicable to IONPs from green synthesis. Labeling IONPs from green synthesis with approved fungicidal drugs should also be viable, allowing for more targeted delivery with dual antifungal effects. However, studies using this strategy are currently insufficient, and the safety of such modified IONPs will need to be carefully investigated [240].

The mechanism of action of IONPs for their antifungal activity has not been investigated in detail; however, it is expected to involve the same mechanisms that are responsible for their antibacterial activity. This includes the effects on cell membrane permeability and the generation of radical oxygen species (ROS) via Fenton reactions or photocatalytic reactions with dissolved oxygen, which cause damage to the cell's DNA, cell wall components, and proteins, resulting in cell growth inhibition and cell death. The nanoparticles' high surface-to-volume ratio allows them to strongly adhere to the cell surface of fungi, while their small size allows them to penetrate and damage the cell wall, directing their effects toward the microbial cells [105]. To fully understand the mechanism of action for the antimycotic activity of IONPs derived from green synthesis, more research will be

Preprints (www.preprints.org) | NOT PEER-REVIEWED | Posted: 3 October 2023 doi:10.20944/preprints202310.0123.v1

required, which will also help us better understand the different activity profiles of varying IONPs against different fungal strains.

A summary of the described studies is provided in Table 8 and reveals that the antimicrobial activity of IONPs generated by green synthesis can vary depending on the biological source material and synthesis approach used.

Table 8. Antifungal activity of iron oxide nanoparticles derived from green synthesis.

Treated fungal strain	Biological source for IONP generation	Approach	Size (nm)	Nanoparticle morphology	Inhibition zone (mm)	Ref.
Alternaria alternata	-	Tannic acid	10–30	quasi circular	21.33 ± 3.83	[236]
Arthogrophis cuboida	*Euphorbia hirta*	Leaf extract	25 – 80	Cavity like structures	25.33 ± 0.5	[94]
Aspergillus flavus	*Laurus nobilis* L.	Leaf extract	8.03 ± 8.99	crystalline, spherical; partly hexagonal	13	[3]
	Green Tea (GT) or black Tea (BT)	Leaf extract	42–60	agglomerated & spherical	Aflatoxin reduction [%]: GT: 43.5 ± 1.5 BT: 39.2 ± 0.9	[237]
Aspergillus fumigatus	*Euphorbia hirta*	Leaf extract	25 – 80	Cavity like structures	21.67 ± 1.5	[94]
Aspergillus niger	-	Tannic acid	10–30	circular	26.33 ± 1.15	[236]
	Platanus orientalis	Leaf extract	38	spherical	16	[105]
	Euphorbia hirta	Leaf extract	25 – 80	Cavity like structures	18.67 ± 0.5	[94]
Aspergillus parasiticus	Green Tea (GT) or Black Tea (BT)	Leaf extract	42–60	agglomerated & spherical	Aflatoxin reduction [%]: GT: 51.6 ± 1.6 BT: 47.1 ± 3.1	[237]
Cladosporium herbarum	-	Tannic acid	10–30	circular	18.00 ± 1.00	[236]
	Euphorbia helioscopia	Leaf extract	7 – 10	spherical	38.33	[238]
Mucor piriformis	*Platanus orientalis*	Leaf extract	38	spherical	26	[105]
Penicillium chrysogenum	-	Tannic acid	10–30	circular	28.67 ± 1.53	[236]
Penicillium spinulosum	*Laurus nobilis* L.	Leaf extract	8.03 ± 8.99	crystalline, spherical; partly hexagonal	14	[3]
Trichothecium roseum	-	Tannic acid	10–30	circular	22.67 ± 2.52	[236]

4.3. Antiparasitic activity

IONPs derived either from green or chemical synthesis have been used as antiplasmodial and antileishmanial agents; however, most studies have used chemically synthesized NPs [241] [242], and only few reports exist of the use of green synthesized IONPs (Table 9). Furthermore, the IONPs have

Preprints (www.preprints.org) | NOT PEER-REVIEWED | Posted: 3 October 2023 doi:10.20944/preprints202310.0123.v1

been used in combination with known antiparasitic drugs (i.e., artesunate, albendazole) to enhance their inhibitory effect [242-244]. Nevertheless, to the best of our knowledge, none of the studies have used green synthesized IONPs. A key feature is that IONPs have not shown cytotoxic effects *in vitro*, making them attractive for pharmaceutical and medical applications [14].

When the antileishmanial activity (IC_{50}) of chemically synthesized IONPs was compared to that of biologically synthesized IONPs from *Trigonella foenum-graecum* plant extract, no greater difference against both promastigotes and amastigotes of *Leishmania tropica* was observed, despite the fact that the IC_{50}s of biologically synthesized IONPs were slightly lower. However, an enhanced inhibitory effect was observed under LED exposure [245]. High levels of reactive oxygen species were found to be responsible for parasite DNA damage and membrane integrity loss. Notably, these green synthesized IONPs proved to be biocompatible with human erythrocytes. Overall, the results showed that biologically produced IONPs had promising antiprotozoal agent capabilities [245]. In another study, IONPs synthesized from $FeCl_3.6H_2O$ and *Nephrolepis exaltata* aqueous extract showed favorable parasite inhibitory activity against Plasmodium at 25 µg/mL (62 % inhibition) when compared to chloroquine control samples (70 % inhibition) at the same concentration [14]; however, the mechanism of action was not described.

In general, these IONPs show encouraging antiparasitic properties. Nevertheless, most studies (although limited) are based on non-green synthesized IONPs. As a result, further research should be done using IONPs obtained through green synthesis to better understand their potential to inhibit parasite growth.

Table 9. List of studies using iron oxide nanoparticles (IONPs) derived from green synthesis as antiparasitic or antiviral agents.

Treated microorganism	Biological source for IONP generation	Approach	Size (nm)	Nanoparticle morphology	Ref.
		Parasites			
Plasmodium	*Nephrolepis exaltata*	IONPs alone	16	Roughly spherical	[14]
Leishmania tropica KWH23	*Trigonella foenum-graecum*	Synergistic effects of IONPs and LED light together	-	-	[245]
		Virus			
Poliovirus (Type 1 and 3)	*Hyphaene thebaica*	IONPs alone	10	Quasi-spherical and cuboidal	[246]

4.4. Antiviral activity

Nanotechnology and its applications have shown great potential in the development of novel diagnostic and therapeutic approaches against viral infections [247]. In particular, literature has reported exciting discoveries regarding the antiviral activity of metal complexes and metal-based nanomaterials [248]. Most of these studies involve both the use of the nanoparticles alone or the coating of nanoparticle surfaces with known antiviral compounds [249,250]. The main antiviral mechanisms observed in metal and metal oxide nanoparticles are: inhibition of viral attachment and uncoating by viral-attachment-protein hijacking, disruption of glycoprotein disulfide bonds, and viral structure denaturation via oxidation (reactive oxygen species or ROS) [4]. However, the study of iron oxide nanoparticles (IONPs) has received little attention as potential antivirals. Chemically synthesized IONPs had antiviral activity against the H1N1 Influenza A virus [251,252]. The use of approximately 4.25 pg of IONPs reduced viral titer by 8-fold while maintaining 50% of cell viability [252]. However, the human and environmental effects of the inherent toxicity associated with laboratory chemical synthesis and its byproducts are a serious issue [253]. A recent study described

 doi:10.20944/preprints202310.0123.v1

a moderate inhibition of polio virus-1 and polio virus-2 after treatment of infected L20B (mice cell line transfected with poliovirus receptor) and RD (human rhabdomyosarcoma) cells with IONPs synthesized from the aqueous fruit extracts of *Hyphaene thebaica* (Table 9) [246]. Overall, the antiviral potential of IONPs is vast and still remains unexplored, which poses a fundamental question to be fulfilled by future studies regarding green-synthesized nanoparticles.

5. Conclusions and future prospects

The present review provides a thorough examination of Iron Oxide Nanoparticles (IONPs), specifically focusing on their synthesis through environmentally sustainable methods, their notable antimicrobial capabilities, and the significance of the most prominent characterization methods. This combination of factors sheds light on both the potential benefits and challenges associated with the utilization of IONPs as antimicrobial agents.

The green synthesis of IONPs, frequently involving the utilization of plant extracts, microorganisms, or biocompatible materials, aligns cohesively with the contemporary emphasis on sustainability and eco-friendly practices within the realm of nanotechnology. Such an environmentally conscious approach not only minimizes the ecological footprint but also engenders the development of nanomaterials that are safer and more biocompatible.

The demonstrated antimicrobial efficacy of IONPs, spanning a broad spectrum of microorganisms encompassing bacteria, fungi, parasites and viruses, represents a promising avenue for addressing the escalating global challenge of antimicrobial resistance. The observed synergistic effects when IONPs are combined with traditional antibiotics present a potential solution for countering resistant strains.

Nevertheless, it is imperative to acknowledge and confront the constraints and apprehensions surrounding the use of IONPs. Cytotoxicity remains a substantial challenge, necessitating meticulous optimization of dosage, surface functionalization, and comprehensive assessments of biocompatibility. Furthermore, the long-term consequences of IONPs exposure and the prospect of their accumulation in biological systems demand further rigorous investigation.

Looking forward, the prospects of IONPs as antimicrobial agents appear promising. Advancements in surface modification techniques, innovative strategies for targeted delivery, and rigorous regulatory approval procedures are poised to unlock their full potential. Additionally, mindful consideration of their potential environmental implications and the implementation of responsible disposal methodologies are integral components of future research and applications.

In essence, the combination of green synthesis methodologies, potent antimicrobial attributes, and rigorous characterization of IONPs has unveiled a promising trajectory for combating microbial infections. While challenges persist, the convergence of research endeavors, accompanied by an unwavering commitment to safety and sustainability, offers a glimpse into a future where IONPs stand poised to revolutionize the landscape of antimicrobial therapeutics, thereby mitigating the escalating global threat of antimicrobial resistance.

Author Contributions: Conceptualization J.Z.-M.; writing—original draft preparation J.Z.-M., J.G., J.H.-M., C.B.-O., S.E.C.-P., A.M., A.M.-R., L.P.-G, writing—review and editing J.Z.-M., J.G., J.H.-M., C.B.-O., S.E.C.-P., A.M., A.M.-R., L.P.-G; supervision J.Z.-M.; project administration J.Z.-M, L.P.-G. All authors have read and agreed to the published version of the manuscript.
Funding: This research received no external funding.
Institutional Review Board Statement: Not applicable.
Informed Consent Statement: Not applicable.
Data Availability Statement: All tables were created by the authors. All sources of information were adequately referenced. There was no need to obtain copyright permission.
Acknowledgments: All the figures in the article were created with Biorender.com
Conflicts of Interest: The authors declare no conflict of interest

References

1. Aisida, S.O.; Madubuonu, N.; Alnasir, M.H.; Ahmad, I.; Botha, S.; Maaza, M.; Ezema, F.I. Biogenic synthesis of iron oxide nanorods using Moringa oleifera leaf extract for antibacterial applications. *Appl. Nanosci.* **2020**, *10*, 305–315, doi:10.1007/s13204-019-01099-x.
2. Hussain, I.; Singh, N.B.; Singh, A.; Singh, H.; Singh, S.C. Green synthesis of nanoparticles and its potential application. *Biotechnol. Lett.* **2016**, *38*, 545–560, doi:10.1007/s10529-015-2026-7.
3. Jamzad, M.; Kamari Bidkorpeh, M. Green synthesis of iron oxide nanoparticles by the aqueous extract of Laurus nobilis L. leaves and evaluation of the antimicrobial activity. *J. Nanostruct. Chem.* **2020**, *10*, 193–201, doi:10.1007/s40097-020-00341-1.
4. Alavi, M.; Kamarasu, P.; McClements, D.J.; Moore, M.D. Metal and metal oxide-based antiviral nanoparticles: Properties, mechanisms of action, and applications. *Adv. Colloid Interface Sci.* **2022**, *306*, 102726, doi:10.1016/j.cis.2022.102726.
5. Gao, L.; Fan, K.; Yan, X. Iron oxide nanozyme: A multifunctional enzyme mimetic for biomedical applications. *Theranostics* **2017**, *7*, 3207–3227, doi:10.7150/thno.19738.
6. Bhuiyan, M.S.H.; Miah, M.Y.; Paul, S.C.; Aka, T.D.; Saha, O.; Rahaman, M.M.; Sharif, M.J.I.; Habiba, O.; Ashaduzzaman, M. Green synthesis of iron oxide nanoparticle using Carica papaya leaf extract: application for photocatalytic degradation of remazol yellow RR dye and antibacterial activity. *Heliyon* **2020**, *6*, e04603, doi:10.1016/j.heliyon.2020.e04603.
7. Siddiqi, K.S.; Ur Rahman, A.; Tajuddin; Husen, A. Biogenic fabrication of iron/iron oxide nanoparticles and their application. *Nanoscale Res. Lett.* **2016**, *11*, 498, doi:10.1186/s11671-016-1714-0.
8. Ali, A.; Zafar, H.; Zia, M.; Ul Haq, I.; Phull, A.R.; Ali, J.S.; Hussain, A. Synthesis, characterization, applications, and challenges of iron oxide nanoparticles. *Nanotechnol. Sci. Appl.* **2016**, *9*, 49–67, doi:10.2147/NSA.S99986.
9. Singh, P.; Kim, Y.-J.; Zhang, D.; Yang, D.-C. Biological Synthesis of Nanoparticles from Plants and Microorganisms. *Trends Biotechnol.* **2016**, *34*, 588–599, doi:10.1016/j.tibtech.2016.02.006.
10. Priya; Naveen; Kaur, K.; Sidhu, A.K. Green Synthesis: An Eco-friendly Route for the Synthesis of Iron Oxide Nanoparticles. *Front. Nanotechnol.* **2021**, *3*, doi:10.3389/fnano.2021.655062.
11. Lahiri, D.; Nag, M.; Sheikh, H.I.; Sarkar, T.; Edinur, H.A.; Pati, S.; Ray, R.R. Microbiologically-Synthesized Nanoparticles and Their Role in Silencing the Biofilm Signaling Cascade. *Front. Microbiol.* **2021**, *12*, 636588, doi:10.3389/fmicb.2021.636588.
12. Fatemi, M.; Mollania, N.; Momeni-Moghaddam, M.; Sadeghifar, F. Extracellular biosynthesis of magnetic iron oxide nanoparticles by Bacillus cereus strain HMH1: Characterization and in vitro cytotoxicity analysis on MCF-7 and 3T3 cell lines. *J. Biotechnol.* **2018**, *270*, 1–11, doi:10.1016/j.jbiotec.2018.01.021.
13. Nadeem, M.; Khan, R.; Shah, N.; Bangash, I.R.; Abbasi, B.H.; Hano, C.; Liu, C.; Ullah, S.; Hashmi, S.S.; Nadhman, A.; Celli, J. A review of microbial mediated iron nanoparticles (ionps) and its biomedical applications. *Nanomaterials (Basel)* **2021**, *12*, doi:10.3390/nano12010130.
14. Nadeem, F.; Fozia, F.; Aslam, M.; Ahmad, I.; Ahmad, S.; Ullah, R.; Almutairi, M.H.; Aleya, L.; Abdel-Daim, M.M. Characterization, Antiplasmodial and Cytotoxic Activities of Green Synthesized Iron Oxide Nanoparticles Using Nephrolepis exaltata Aqueous Extract. *Molecules* **2022**, *27*, doi:10.3390/molecules27154931.
15. Iravani, S.; Varma, R.S. Greener synthesis of lignin nanoparticles and their applications. *Green Chem.* **2020**, *22*, 612–636, doi:10.1039/C9GC02835H.
16. Fani, M.; Ghandehari, F.; Rezaee, M. Biosynthesis of Iron Oxide Nanoparticles by Cytoplasmic Extract of Bacteria Lactobacillus Fermentum. *Journal of Medicinal and Chemical Sciences* **2018**.
17. Sundaram, P.A.; Augustine, R.; Kannan, M. Extracellular biosynthesis of iron oxide nanoparticles by Bacillus subtilis strains isolated from rhizosphere soil. *Biotechnol. Bioprocess Eng.* **2012**, *17*, 835–840, doi:10.1007/s12257-011-0582-9.
18. Torabian, P.; Ghandehari, F.; Fatemi, M. Biosynthesis of iron oxide nanoparticles by cytoplasmic extracts of bacteria lactobacillus casei. *Asian Journal of Green Chemistry* **2018**.
19. Dlamini, N.G.; Basson, A.K.; Pullabhotla, R.V. Wastewater Treatment by a Polymeric Bioflocculant and Iron Nanoparticles Synthesized from a Bioflocculant. *Polymers (Basel)* **2020**, *12*, doi:10.3390/polym12071618.
20. Bharde, A.A.; Parikh, R.Y.; Baidakova, M.; Jouen, S.; Hannoyer, B.; Enoki, T.; Prasad, B.L.V.; Shouche, Y.S.; Ogale, S.; Sastry, M. Bacteria-mediated precursor-dependent biosynthesis of superparamagnetic iron oxide and iron sulfide nanoparticles. *Langmuir* **2008**, *24*, 5787–5794, doi:10.1021/la704019p.
21. Bharde, A.; Wani, A.; Shouche, Y.; Joy, P.A.; Prasad, B.L.V.; Sastry, M. Bacterial aerobic synthesis of nanocrystalline magnetite. *J. Am. Chem. Soc.* **2005**, *127*, 9326–9327, doi:10.1021/ja0508469.
22. Kaul, R.K.; Kumar, P.; Burman, U.; Joshi, P.; Agrawal, A.; Raliya, R.; Tarafdar, J.C. Magnesium and iron nanoparticles production using microorganisms and various salts. *Mater Sci-Pol* **2012**, *30*, 254–258, doi:10.2478/s13536-012-0028-x.
23. Daneshvar, M.; Hosseini, M.R. From the iron boring scraps to superparamagnetic nanoparticles through an aerobic biological route. *J. Hazard. Mater.* **2018**, *357*, 393–400, doi:10.1016/j.jhazmat.2018.06.024.

24. Das, K.R.; Kerkar, S. Biosynthesis of iron nanoparticles by sulphate reducing bacteria and its application in remediating chromium from water. *Int. J. Pharma Bio Sci.* **2017**, *8*, doi:10.22376/ijpbs.2017.8.4.b538-546.
25. Crespo, K.A.; Baronetti, J.L.; Quinteros, M.A.; Páez, P.L.; Paraje, M.G. Intra- and Extracellular Biosynthesis and Characterization of Iron Nanoparticles from Prokaryotic Microorganisms with Anticoagulant Activity. *Pharm. Res.* **2017**, *34*, 591–598, doi:10.1007/s11095-016-2084-0.
26. Byrne, J.M.; Telling, N.D.; Coker, V.S.; Pattrick, R.A.D.; van der Laan, G.; Arenholz, E.; Tuna, F.; Lloyd, J.R. Control of nanoparticle size, reactivity and magnetic properties during the bioproduction of magnetite by Geobacter sulfurreducens. *Nanotechnology* **2011**, *22*, 455709, doi:10.1088/0957-4484/22/45/455709.
27. Arias, S.L.; Shetty, A.R.; Senpan, A.; Echeverry-Rendón, M.; Reece, L.M.; Allain, J.P. Fabrication of a Functionalized Magnetic Bacterial Nanocellulose with Iron Oxide Nanoparticles. *J. Vis. Exp.* **2016**, doi:10.3791/52951.
28. Raĭkher, Yu.L.; Stepanov, V.I.; Stolyar, S.V.; Ladygina, V.P.; Balaev, D.A.; Ishchenko, L.A.; Balasoiu, M. Magnetic properties of biomineral particles produced by bacteria Klebsiella oxytoca. *Phys. Solid State* **2010**, *52*, 298–305, doi:10.1134/S1063783410020125.
29. Hashimoto, H.; Yokoyama, S.; Asaoka, H.; Kusano, Y.; Ikeda, Y.; Seno, M.; Takada, J.; Fujii, T.; Nakanishi, M.; Murakami, R. Characteristics of hollow microtubes consisting of amorphous iron oxide nanoparticles produced by iron oxidizing bacteria, Leptothrix ochracea. *J. Magn. Magn. Mater.* **2007**, *310*, 2405–2407, doi:10.1016/j.jmmm.2006.10.793.
30. Obayemi, J.D.; Dozie-Nwachukwu, S.; Danyuo, Y.; Odusanya, O.S.; Anuku, N.; Malatesta, K.; Soboyejo, W.O. Biosynthesis and the conjugation of magnetite nanoparticles with luteinizing hormone releasing hormone (LHRH). *Mater. Sci. Eng. C Mater. Biol. Appl.* **2015**, *46*, 482–496, doi:10.1016/j.msec.2014.10.081.
31. Rosenfeldt, S.; Mickoleit, F.; Jörke, C.; Clement, J.H.; Markert, S.; Jérôme, V.; Schwarzinger, S.; Freitag, R.; Schüler, D.; Uebe, R.; Schenk, A.S. Towards standardized purification of bacterial magnetic nanoparticles for future in vivo applications. *Acta Biomater.* **2021**, *120*, 293–303, doi:10.1016/j.actbio.2020.07.042.
32. Mukherjee, P. Stenotrophomonas and microbacterium: mediated biogenesis of copper, silver and iron nanoparticles—proteomic insights and antibacterial properties versus biofilm formation. *J. Clust. Sci.* **2017**, *28*, 331–358, doi:10.1007/s10876-016-1097-5.
33. Li, J.; Menguy, N.; Gatel, C.; Boureau, V.; Snoeck, E.; Patriarche, G.; Leroy, E.; Pan, Y. Crystal growth of bullet-shaped magnetite in magnetotactic bacteria of the Nitrospirae phylum. *J. R. Soc. Interface* **2015**, *12*, doi:10.1098/rsif.2014.1288.
34. Desai, M.P.; Pawar, K.D. Immobilization of cellulase on iron tolerant Pseudomonas stutzeri biosynthesized photocatalytically active magnetic nanoparticles for increased thermal stability. *Mater. Sci. Eng. C Mater. Biol. Appl.* **2020**, *106*, 110169, doi:10.1016/j.msec.2019.110169.
35. de França Bettencourt, G.M.; Degenhardt, J.; Zevallos Torres, L.A.; de Andrade Tanobe, V.O.; Soccol, C.R. Green biosynthesis of single and bimetallic nanoparticles of iron and manganese using bacterial auxin complex to act as plant bio-fertilizer. *Biocatal. Agric. Biotechnol.* **2020**, *30*, 101822, doi:10.1016/j.bcab.2020.101822.
36. Zaki, S.A.; Eltarahony, M.M.; Abd-El-Haleem, D.A. Disinfection of water and wastewater by biosynthesized magnetite and zerovalent iron nanoparticles via NAP-NAR enzymes of Proteus mirabilis 10B. *Environ. Sci. Pollut. Res. Int.* **2019**, *26*, 23661–23678, doi:10.1007/s11356-019-05479-2.
37. Bose, S.; Hochella, M.F.; Gorby, Y.A.; Kennedy, D.W.; McCready, D.E.; Madden, A.S.; Lower, B.H. Bioreduction of hematite nanoparticles by the dissimilatory iron reducing bacterium Shewanella oneidensis MR-1. *Geochim. Cosmochim. Acta* **2009**, *73*, 962–976, doi:10.1016/j.gca.2008.11.031.
38. Haikarainen, T.; Paturi, P.; Lindén, J.; Haataja, S.; Meyer-Klaucke, W.; Finne, J.; Papageorgiou, A.C. Magnetic properties and structural characterization of iron oxide nanoparticles formed by Streptococcus suis Dpr and four mutants. *J. Biol. Inorg. Chem.* **2011**, *16*, 799–807, doi:10.1007/s00775-011-0781-z.
39. Moon, J.-W.; Rawn, C.J.; Rondinone, A.J.; Love, L.J.; Roh, Y.; Everett, S.M.; Lauf, R.J.; Phelps, T.J. Large-scale production of magnetic nanoparticles using bacterial fermentation. *J. Ind. Microbiol. Biotechnol.* **2010**, *37*, 1023–1031, doi:10.1007/s10295-010-0749-y.
40. Elcey; Kuruvilla, A.; Thomas, D. Synthesis of magnetite nanoparticles from optimized iron reducing bacteria isolated from iron ore mining sites. *undefined* **2014**.
41. Chatterjee, S.; Mahanty, S.; Das, P.; Chaudhuri, P.; Das, S. Biofabrication of iron oxide nanoparticles using manglicolous fungus Aspergillus niger BSC-1 and removal of Cr(VI) from aqueous solution. *Chemical Engineering Journal* **2020**, *385*, 123790, doi:10.1016/j.cej.2019.123790.
42. Bharde, A.; Rautaray, D.; Bansal, V.; Ahmad, A.; Sarkar, I.; Yusuf, S.M.; Sanyal, M.; Sastry, M. Extracellular biosynthesis of magnetite using fungi. *Small* **2006**, *2*, 135–141, doi:10.1002/smll.200500180.
43. Agarwal, H.; Venkat Kumar, S.; Rajeshkumar, S. A review on green synthesis of zinc oxide nanoparticles – An eco-friendly approach. *Resource-Efficient Technologies* **2017**, *3*, 406–413, doi:10.1016/j.reffit.2017.03.002.
44. Alghuthaymi, M.A.; Almoammar, H.; Rai, M.; Said-Galiev, E.; Abd-Elsalam, K.A. Myconanoparticles: synthesis and their role in phytopathogens management. *Biotechnol. Biotechnol. Equip.* **2015**, *29*, 221–236, doi:10.1080/13102818.2015.1008194.

45. Zakariya, N.A.; Majeed, S.; Jusof, W.H.W. Investigation of antioxidant and antibacterial activity of iron oxide nanoparticles (IONPS) synthesized from the aqueous extract of Penicillium spp. *Sensors International* **2022**, *3*, 100164, doi:10.1016/j.sintl.2022.100164.
46. Wang, L.; Liu, X.; Lee, D.-J.; Tay, J.-H.; Zhang, Y.; Wan, C.-L.; Chen, X.-F. Recent advances on biosorption by aerobic granular sludge. *J. Hazard. Mater.* **2018**, *357*, 253–270, doi:10.1016/j.jhazmat.2018.06.010.
47. Silva, L.P.; Reis, I.G.; Bonatto, C.C. Green synthesis of metal nanoparticles by plants: current trends and challenges. In *Green processes for nanotechnology*; Basiuk, V. A., Basiuk, E. V., Eds.; Springer International Publishing: Cham, 2015; pp. 259–275 ISBN 978-3-319-15460-2.
48. Bhargava, A.; Jain, N.; Barathi L., M.; Akhtar, Mohd.S.; Yun, Y.-S.; Panwar, J. Synthesis, characterization and mechanistic insights of mycogenic iron oxide nanoparticles. In *Nanotechnology for sustainable development*; Diallo, M. S., Fromer, N. A., Jhon, M. S., Eds.; Springer International Publishing: Cham, 2014; pp. 337–348 ISBN 978-3-319-05040-9.
49. Mahanty, S.; Bakshi, M.; Ghosh, S.; Chatterjee, S.; Bhattacharyya, S.; Das, P.; Das, S.; Chaudhuri, P. Green Synthesis of Iron Oxide Nanoparticles Mediated by Filamentous Fungi Isolated from Sundarban Mangrove Ecosystem, India. *Bionanoscience* **2019**, *9*, 637–651, doi:10.1007/s12668-019-00644-w.
50. Baccile, N.; Noiville, R.; Stievano, L.; Van Bogaert, I. Sophorolipids-functionalized iron oxide nanoparticles. *Phys. Chem. Chem. Phys.* **2013**, *15*, 1606–1620, doi:10.1039/c2cp41977g.
51. Sarkar, J.; Mollick, M.M.R.; Chattopadhyay, D.; Acharya, K. An eco-friendly route of γ-Fe2O3 nanoparticles formation and investigation of the mechanical properties of the HPMC-γ-Fe2O3 nanocomposites. *Bioprocess Biosyst. Eng.* **2017**, *40*, 351–359, doi:10.1007/s00449-016-1702-x.
52. Abdeen, M.; Sabry, S.; Ghozlan, H.; El-Gendy, A.A.; Carpenter, E.E. Microbial-Physical Synthesis of Fe and Fe_3O_4 Magnetic Nanoparticles Using*Aspergillus niger* YESM1 and Supercritical Condition of Ethanol. *J. Nanomater.* **2016**, *2016*, 1–7, doi:10.1155/2016/9174891.
53. Mishra, A.; Ahmad, R.; Sardar, M. Biosynthesized iron oxide nanoparticles mimicking peroxidase activity: application for biocatalysis and biosensing. *J Nanoengng Nanomfg* **2015**, *5*, 37–42, doi:10.1166/jnan.2015.1220.
54. Vainshtein, M.; Belova, N.; Kulakovskaya, T.; Suzina, N.; Sorokin, V. Synthesis of magneto-sensitive iron-containing nanoparticles by yeasts. *J. Ind. Microbiol. Biotechnol.* **2014**, *41*, 657–663, doi:10.1007/s10295-014-1417-4.
55. Li, Q.; Liu, D.; Wang, T.; Chen, C.; Gadd, G.M. Iron coral: Novel fungal biomineralization of nanoscale zerovalent iron composites for treatment of chlorinated pollutants. *Chemical Engineering Journal* **2020**, *402*, 126263, doi:10.1016/j.cej.2020.126263.
56. Fawcett, D.; Verduin, J.J.; Shah, M.; Sharma, S.B.; Poinern, G.E.J. A Review of Current Research into the Biogenic Synthesis of Metal and Metal Oxide Nanoparticles via Marine Algae and Seagrasses. *Journal of Nanoscience* **2017**, *2017*, 1–15, doi:10.1155/2017/8013850.
57. de Morais, M.G.; Vaz, B. da S.; de Morais, E.G.; Costa, J.A.V. Biologically active metabolites synthesized by microalgae. *Biomed Res. Int.* **2015**, *2015*, 835761, doi:10.1155/2015/835761.
58. Mahdavi, M.; Namvar, F.; Ahmad, M.B.; Mohamad, R. Green biosynthesis and characterization of magnetic iron oxide (Fe_3O_4) nanoparticles using seaweed (Sargassum muticum) aqueous extract. *Molecules* **2013**, *18*, 5954–5964, doi:10.3390/molecules18055954.
59. Sathishkumar, R.S.; Sundaramanickam, A.; Srinath, R.; Ramesh, T.; Saranya, K.; Meena, M.; Surya, P. Green synthesis of silver nanoparticles by bloom forming marine microalgae Trichodesmium erythraeum and its applications in antioxidant, drug-resistant bacteria, and cytotoxicity activity. *Journal of Saudi Chemical Society* **2019**, *23*, 1180–1191, doi:10.1016/j.jscs.2019.07.008.
60. Subramaniyam, V.; Subashchandrabose, S.R.; Ganeshkumar, V.; Thavamani, P.; Chen, Z.; Naidu, R.; Megharaj, M. Cultivation of Chlorella on brewery wastewater and nano-particle biosynthesis by its biomass. *Bioresour. Technol.* **2016**, *211*, 698–703, doi:10.1016/j.biortech.2016.03.154.
61. Salem, D.M.S.A.; Ismail, M.M.; Aly-Eldeen, M.A. Biogenic synthesis and antimicrobial potency of iron oxide (Fe3O4) nanoparticles using algae harvested from the Mediterranean Sea, Egypt. *The Egyptian Journal of Aquatic Research* **2019**, *45*, 197–204, doi:10.1016/j.ejar.2019.07.002.
62. Sandhya, J.; Kalaiselvam, S. Biogenic synthesis of magnetic iron oxide nanoparticles using inedible borassus flabellifer seed coat: characterization, antimicrobial, antioxidant activity and *in vitro* cytotoxicity analysis. *Mater. Res. Express* **2020**, *7*, 015045, doi:10.1088/2053-1591/ab6642.
63. Sicard, C.; Brayner, R.; Margueritat, J.; Hémadi, M.; Couté, A.; Yéprémian, C.; Djediat, C.; Aubard, J.; Fiévet, F.; Livage, J.; Coradin, T. Nano-gold biosynthesis by silica-encapsulated micro-algae: a "living" bio-hybrid material. *J. Mater. Chem.* **2010**, *20*, 9342, doi:10.1039/c0jm01735c.
64. Siji, S.; Njana, J.; AmritaP, J.; Vishnudasan, D. Biogenic Synthesis of Iron oxide Nanoparticles from Marine Algae. **2018**.
65. Win, T.T.; Khan, S.; Bo, B.; Zada, S.; Fu, P. Green synthesis and characterization of Fe3O4 nanoparticles using Chlorella-K01 extract for potential enhancement of plant growth stimulating and antifungal activity. *Sci. Rep.* **2021**, *11*, 21996, doi:10.1038/s41598-021-01538-2.

66. El-Sheekh, M.M.; El-Kassas, H.Y.; Shams El-Din, N.G.; Eissa, D.I.; El-Sherbiny, B.A. Green synthesis, characterization applications of iron oxide nanoparticles for antialgal and wastewater bioremediation using three brown algae. *Int. J. Phytoremediation* **2021**, *23*, 1538–1552, doi:10.1080/15226514.2021.1915957.
67. Yew, Y.P.; Shameli, K.; Miyake, M.; Kuwano, N.; Bt Ahmad Khairudin, N.B.; Bt Mohamad, S.E.; Lee, K.X. Green Synthesis of Magnetite (Fe3O4) Nanoparticles Using Seaweed (Kappaphycus alvarezii) Extract. *Nanoscale Res. Lett.* **2016**, *11*, 276, doi:10.1186/s11671-016-1498-2.
68. Arularasu, M.V.; Devakumar, J.; Rajendran, T.V. An innovative approach for green synthesis of iron oxide nanoparticles: Characterization and its photocatalytic activity. *Polyhedron* **2018**, *156*, 279–290, doi:10.1016/j.poly.2018.09.036.
69. El-Kassas, H.Y.; Aly-Eldeen, M.A.; Gharib, S.M. Green synthesis of iron oxide (Fe3O4) nanoparticles using two selected brown seaweeds: Characterization and application for lead bioremediation. *Acta Oceanol. Sin.* **2016**, *35*, 89–98, doi:10.1007/s13131-016-0880-3.
70. Shalaby, S.M.; Madkour, F.F.; El-Kassas, H.Y.; Mohamed, A.A.; Elgarahy, A.M. Green synthesis of recyclable iron oxide nanoparticles using Spirulina platensis microalgae for adsorptive removal of cationic and anionic dyes. *Environ. Sci. Pollut. Res. Int.* **2021**, *28*, 65549–65572, doi:10.1007/s11356-021-15544-4.
71. Bibi, I.; Nazar, N.; Ata, S.; Sultan, M.; Ali, A.; Abbas, A.; Jilani, K.; Kamal, S.; Sarim, F.M.; Khan, M.I.; Jalal, F.; Iqbal, M. Green synthesis of iron oxide nanoparticles using pomegranate seeds extract and photocatalytic activity evaluation for the degradation of textile dye. *Journal of Materials Research and Technology* **2019**, *8*, 6115–6124, doi:10.1016/j.jmrt.2019.10.006.
72. Saif, S.; Tahir, A.; Chen, Y. Green synthesis of iron nanoparticles and their environmental applications and implications. *Nanomaterials (Basel)* **2016**, *6*, doi:10.3390/nano6110209.
73. Bolade, O.P.; Williams, A.B.; Benson, N.U. Green synthesis of iron-based nanomaterials for environmental remediation: A review. *Environmental Nanotechnology, Monitoring & Management* **2020**, *13*, 100279, doi:10.1016/j.enmm.2019.100279.
74. Makarov, V.V.; Makarova, S.S.; Love, A.J.; Sinitsyna, O.V.; Dudnik, A.O.; Yaminsky, I.V.; Taliansky, M.E.; Kalinina, N.O. Biosynthesis of stable iron oxide nanoparticles in aqueous extracts of Hordeum vulgare and Rumex acetosa plants. *Langmuir* **2014**, *30*, 5982–5988, doi:10.1021/la5011924.
75. Karunakaran, S.; Ramanujam, S.; Gurunathan, B. Green synthesised iron and iron-based nanoparticle in environmental and biomedical application: - a review. *IET Nanobiotechnol.* **2018**, *12*, 1003–1008, doi:10.1049/iet-nbt.2018.5048.
76. Singh, K.K.; Senapati, K.K.; Sarma, K.C. Synthesis of superparamagnetic Fe 3 O 4 nanoparticles coated with green tea polyphenols and their use for removal of dye pollutant from aqueous solution. *Journal of Environmental Chemical Engineering* **2017**, *5*, 2214–2221, doi:10.1016/j.jece.2017.04.022.
77. Prasad, A.S. Iron oxide nanoparticles synthesized by controlled bio-precipitation using leaf extract of Garlic Vine (Mansoa alliacea). *Mater. Sci. Semicond. Process.* **2016**, *53*, 79–83, doi:10.1016/j.mssp.2016.06.009.
78. Herrera-Becerra, R.; Zorrilla, C.; Ascencio, J.A. Production of iron oxide nanoparticles by a biosynthesis method: an environmentally friendly route. *J. Phys. Chem. C* **2007**, *111*, 16147–16153, doi:10.1021/jp072259a.
79. Anwer, Z.; Jamali, A.R.; Khan, W.; Bhatti, J.; Akhter, F.; Batool, M. Green synthesis of active Fe2O3 nanoparticles using Aloe barbadensis and Camellia sinensis for efficient degradation of malachite green and Congo red dye. *Biomass Conv. Bioref.* **2022**, doi:10.1007/s13399-022-03626-3.
80. Narayanan, K.B.; Han, S.S. One-Pot Green Synthesis of Hematite (α-Fe2O3) Nanoparticles by Ultrasonic Irradiation and Their In Vitro Cytotoxicity on Human Keratinocytes CRL-2310. *J. Clust. Sci.* **2016**, *27*, 1763–1775, doi:10.1007/s10876-016-1040-9.
81. Moacă, E.-A.; Watz, C.G.; Flondor Ionescu, D.; Păcurariu, C.; Tudoran, L.B.; Ianoș, R.; Socoliuc, V.; Drăghici, G.-A.; Iftode, A.; Liga, S.; Dragoș, D.; Dehelean, C.A. Biosynthesis of Iron Oxide Nanoparticles: Physico-Chemical Characterization and Their In Vitro Cytotoxicity on Healthy and Tumorigenic Cell Lines. *Nanomaterials (Basel)* **2022**, *12*, doi:10.3390/nano12122012.
82. Karpagavinayagam, P.; Vedhi, C. Green synthesis of iron oxide nanoparticles using Avicennia marina flower extract. *Vacuum* **2019**, *160*, 286–292, doi:10.1016/j.vacuum.2018.11.043.
83. Zambri, N.D.S.; Taib, N.I.; Abdul Latif, F.; Mohamed, Z. Utilization of neem leaf extract on biosynthesis of iron oxide nanoparticles. *Molecules* **2019**, *24*, doi:10.3390/molecules24203803.
84. Sirdeshpande, K.D.; Sridhar, A.; Cholkar, K.M.; Selvaraj, R. Structural characterization of mesoporous magnetite nanoparticles synthesized using the leaf extract of Calliandra haematocephala and their photocatalytic degradation of malachite green dye. *Appl. Nanosci.* **2018**, 1–9, doi:10.1007/s13204-018-0698-8.
85. Singh, K.; Chopra, D.S.; Singh, D.; Singh, N. Optimization and ecofriendly synthesis of iron oxide nanoparticles as potential antioxidant. *Arabian Journal of Chemistry* **2020**, *13*, 9034–9046, doi:10.1016/j.arabjc.2020.10.025.
86. Thakur, S.; Karak, N. One-step approach to prepare magnetic iron oxide/reduced graphene oxide nanohybrid for efficient organic and inorganic pollutants removal. *Mater. Chem. Phys* **2014**, *144*, 425–432, doi:10.1016/j.matchemphys.2014.01.015.

87. Groiss, S.; Selvaraj, R.; Varadavenkatesan, T.; Vinayagam, R. Structural characterization, antibacterial and catalytic effect of iron oxide nanoparticles synthesised using the leaf extract of Cynometra ramiflora. *J. Mol. Struct* **2017**, *1128*, 572–578, doi:10.1016/j.molstruc.2016.09.031.
88. Ruíz-Baltazar, Á. de J.; Reyes-López, S.Y.; Mondragón-Sánchez, M. de L.; Robles-Cortés, A.I.; Pérez, R. Eco-friendly synthesis of Fe3O4 nanoparticles: Evaluation of their catalytic activity in methylene blue degradation by kinetic adsorption models. *Results in Physics* **2019**, *12*, 989–995, doi:10.1016/j.rinp.2018.12.037.
89. Beheshtkhoo, N.; Kouhbanani, M.A.J.; Savardashtaki, A.; Amani, A.M.; Taghizadeh, S. Green synthesis of iron oxide nanoparticles by aqueous leaf extract of Daphne mezereum as a novel dye removing material. *Appl. Phys. A* **2018**, *124*, 363, doi:10.1007/s00339-018-1782-3.
90. Wei, Y.; Fang, Z.; Zheng, L.; Tsang, E.P. Biosynthesized iron nanoparticles in aqueous extracts of Eichhornia crassipes and its mechanism in the hexavalent chromium removal. *Appl. Surf. Sci.* **2017**, *399*, 322–329, doi:10.1016/j.apsusc.2016.12.090.
91. Balamurugan, M.; Saravanan, S.; Soga, T. Synthesis of iron oxide nanoparticles by using *eucalyptus globulus* plant extract. *e-J. Surf. Sci. Nanotech.* **2014**, *12*, 363–367, doi:10.1380/ejssnt.2014.363.
92. Andrade-Zavaleta, K.; Chacon-Laiza, Y.; Asmat-Campos, D.; Raquel-Checca, N. Green Synthesis of Superparamagnetic Iron Oxide Nanoparticles with Eucalyptus globulus Extract and Their Application in the Removal of Heavy Metals from Agricultural Soil. *Molecules* **2022**, *27*, doi:10.3390/molecules27041367.
93. Atarod, M.; Nasrollahzadeh, M.; Sajadi, S.M. Green synthesis of a Cu/reduced graphene oxide/Fe_3O_4 nanocomposite using *Euphorbia wallichii* leaf extract and its application as a recyclable and heterogeneous catalyst for the reduction of 4-nitrophenol and rhodamine B. *RSC Adv.* **2015**, *5*, 91532–91543, doi:10.1039/C5RA17269A.
94. Ahmad, W.; Kumar Jaiswal, K.; Amjad, M. *Euphorbia herita* leaf extract as a reducing agent in a facile green synthesis of iron oxide nanoparticles and antimicrobial activity evaluation. *Inorganic and Nano-Metal Chemistry* **2020**, 1–8, doi:10.1080/24701556.2020.1815062.
95. Karade, V.C.; Parit, S.B.; Dawkar, V.V.; Devan, R.S.; Choudhary, R.J.; Kedge, V.V.; Pawar, N.V.; Kim, J.H.; Chougale, A.D. A green approach for the synthesis of α-Fe2O3 nanoparticles from Gardenia resinifera plant and it's In vitro hyperthermia application. *Heliyon* **2019**, *5*, e02044, doi:10.1016/j.heliyon.2019.e02044.
96. Narayanan, S.; Sathy, B.N.; Mony, U.; Koyakutty, M.; Nair, S.V.; Menon, D. Biocompatible magnetite/gold nanohybrid contrast agents via green chemistry for MRI and CT bioimaging. *ACS Appl. Mater. Interfaces* **2012**, *4*, 251–260, doi:10.1021/am201311c.
97. Plachtová, P.; Medříková, Z.; Zbořil, R.; Tuček, J.; Varma, R.S.; Maršálek, B. Iron and iron oxide nanoparticles synthesized using green tea extract: improved ecotoxicological profile and ability to degrade malachite green. *ACS Sustain. Chem. Eng.* **2018**, *6*, 8679–8687, doi:10.1021/acssuschemeng.8b00986.
98. Razack, S.A.; Suresh, A.; Sriram, S.; Ramakrishnan, G.; Sadanandham, S.; Veerasamy, M.; Nagalamadaka, R.B.; Sahadevan, R. Green synthesis of iron oxide nanoparticles using Hibiscus rosa-sinensis for fortifying wheat biscuits. *SN Appl. Sci.* **2020**, *2*, 898, doi:10.1007/s42452-020-2477-x.
99. Khalil, A.T.; Ovais, M.; Ullah, I.; Ali, M.; Shinwari, Z.K.; Maaza, M. Biosynthesis of iron oxide (Fe_2O_3) nanoparticles via aqueous extracts of*Sageretia thea* (Osbeck.) and their pharmacognostic properties. *Green Chemistry Letters and Reviews* **2017**, *10*, 186–201, doi:10.1080/17518253.2017.1339831.
100. Kanagasubbulakshmi, S.; Kadirvelu, K. Green synthesis of Iron oxide nanoparticles using Lagenaria siceraria and evaluation of its Antimicrobial activity. *Def. Life. Sc. Jl.* **2017**, *2*, 422, doi:10.14429/dlsj.2.12277.
101. Nithya, K.; Sathish, A.; Senthil Kumar, P.; Ramachandran, T. Fast kinetics and high adsorption capacity of green extract capped superparamagnetic iron oxide nanoparticles for the adsorption of Ni(II) ions. *Journal of Industrial and Engineering Chemistry* **2018**, *59*, 230–241, doi:10.1016/j.jiec.2017.10.028.
102. Chauhan, S.; Upadhyay, L.S.B. Biosynthesis of iron oxide nanoparticles using plant derivatives of Lawsonia inermis (Henna) and its surface modification for biomedical application. *Nanotechnol. Environ. Eng.* **2019**, *4*, 8, doi:10.1007/s41204-019-0055-5.
103. Pattanayak, M.; Nayak, P.L. Ecofriendly green synthesis of iron nanoparticles from various plants and spices extract. *International Journal of Plant, Animal and Environmental Sciences* **2013**.
104. Lohrasbi, S.; Kouhbanani, M.A.J.; Beheshtkhoo, N.; Ghasemi, Y.; Amani, A.M.; Taghizadeh, S. Green Synthesis of Iron Nanoparticles Using Plantago major Leaf Extract and Their Application as a Catalyst for the Decolorization of Azo Dye. *Bionanoscience* **2019**, *9*, 1–6, doi:10.1007/s12668-019-0596-x.
105. Devi, H.S.; Boda, M.A.; Shah, M.A.; Parveen, S.; Wani, A.H. Green synthesis of iron oxide nanoparticles using Platanus orientalis leaf extract for antifungal activity. *Green Processing and Synthesis* **2019**, *8*, 38–45, doi:10.1515/gps-2017-0145.
106. Madubuonu, N.; Aisida, S.O.; Ahmad, I.; Botha, S.; Zhao, T.; Maaza, M.; Ezema, F.I. Bio-inspired iron oxide nanoparticles using Psidium guajava aqueous extract for antibacterial activity. *Appl. Phys. A* **2020**, *126*, 72, doi:10.1007/s00339-019-3249-6.
107. Vasantharaj, S.; Sathiyavimal, S.; Senthilkumar, P.; LewisOscar, F.; Pugazhendhi, A. Biosynthesis of iron oxide nanoparticles using leaf extract of Ruellia tuberosa: Antimicrobial properties and their applications

in photocatalytic degradation. *J Photochem Photobiol B, Biol* **2019**, *192*, 74–82, doi:10.1016/j.jphotobiol.2018.12.025.

108. Rajendran, S.P.; Sengodan, K. Synthesis and Characterization of Zinc Oxide and Iron Oxide Nanoparticles Using *Sesbania grandiflora* Leaf Extract as Reducing Agent. *Journal of Nanoscience* **2017**, *2017*, 1–7, doi:10.1155/2017/8348507.
109. Cai, Y.; Shen, Y.; Xie, A.; Li, S.; Wang, X. Green synthesis of soya bean sprouts-mediated superparamagnetic Fe3O4 nanoparticles. *J. Magn. Magn. Mater.* **2010**, *322*, 2938–2943, doi:10.1016/j.jmmm.2010.05.009.
110. Ahmad, W.; Khan, A.U.; Shams, S.; Qin, L.; Yuan, Q.; Ahmad, A.; Wei, Y.; Khan, Z.U.H.; Ullah, S.; Rahman, A.U. Eco-benign approach to synthesize spherical iron oxide nanoparticles: A new insight in photocatalytic and biomedical applications. *J Photochem Photobiol B, Biol* **2020**, *205*, 111821, doi:10.1016/j.jphotobiol.2020.111821.
111. Akhter, S.M.H.; Mohammad, F.; Ahmad, S. Terminalia belerica Mediated Green Synthesis of Nanoparticles of Copper, Iron and Zinc Metal Oxides as the Alternate Antibacterial Agents Against some Common Pathogens. *Bionanoscience* **2019**, *9*, 1–8, doi:10.1007/s12668-019-0601-4.
112. EBSCOhost | 88941904 | Biogenic synthesis of fe3o4 nanoparticles using tridax procumbens leaf extract and its antibacterial activity on pseudomonas aeruginosa. Available online: https://web.p.ebscohost.com/abstract?direct=true&profile=ehost&scope=site&authtype=crawler&jrnl=18423582&asa=Y&AN=88941904&h=NhJp6M8b1WHqokbPkvy5F0nS964DyVei%2fYOlyPXMzZ%2blxWEL%2bup4DlP5C6UyJ0YZzT9E2pRtdXzXFwEIzdyKMQ%3d%3d&crl=c&resultNs=AdminWebAuth&resultLocal=ErrCrlNotAuth&crlhashurl=login.aspx%3fdirect%3dtrue%26profile%3dehost%26scope%3dsite%26authtype%3dcrawler%26jrnl%3d18423582%26asa%3dY%26AN%3d88941904 (accessed on 31 December 2022).
113. Manquián-Cerda, K.; Cruces, E.; Angélica Rubio, M.; Reyes, C.; Arancibia-Miranda, N. Preparation of nanoscale iron (oxide, oxyhydroxides and zero-valent) particles derived from blueberries: Reactivity, characterization and removal mechanism of arsenate. *Ecotoxicol. Environ. Saf.* **2017**, *145*, 69–77, doi:10.1016/j.ecoenv.2017.07.004.
114. Lateef, A.; Oloke, J.K.; Gueguim Kana, E.B.; Oyeniyi, S.O.; Onifade, O.R.; Oyeleye, A.O.; Oladosu, O.C.; Oyelami, A.O. Improving the quality of agro-wastes by solid-state fermentation: enhanced antioxidant activities and nutritional qualities. *World J. Microbiol. Biotechnol.* **2008**, *24*, 2369–2374, doi:10.1007/s11274-008-9749-8.
115. Adelere, I.A.; Lateef, A. A novel approach to the green synthesis of metallic nanoparticles: the use of agro-wastes, enzymes, and pigments. *Nanotechnol. Rev.* **2016**, *5*, doi:10.1515/ntrev-2016-0024.
116. García, D.G.; Garzón-Romero, C.; Salazar, M.A.; Lagos, K.J.; Campaña, K.O.; Debut, A.; Vizuete, K.; Rivera, M.R.; Niebieskikwiat, D.; Benitez, M.J.; Romero, M.P. Bioinspired Synthesis of Magnetic Nanoparticles Based on Iron Oxides Using Orange Waste and Their Application as Photo-Activated Antibacterial Agents. *Int. J. Mol. Sci.* **2023**, *24*, doi:10.3390/ijms24054770.
117. Akpomie, K.G.; Ghosh, S.; Gryzenhout, M.; Conradie, J. Ananas comosus peel–mediated green synthesized magnetite nanoparticles and their antifungal activity against four filamentous fungal strains. *Biomass Conv. Bioref.* **2021**, doi:10.1007/s13399-021-01515-9.
118. Periakaruppan, R.; Chen, X.; Thangaraj, K.; Jeyaraj, A.; Nguyen, H.H.; Yu, Y.; Hu, S.; Lu, L.; Li, X. Utilization of tea resources with the production of superparamagnetic biogenic iron oxide nanoparticles and an assessment of their antioxidant activities. *J. Clean. Prod.* **2021**, *278*, 123962, doi:10.1016/j.jclepro.2020.123962.
119. Elizondo-Villarreal, N.; Verástegui-Domínguez, L.; Rodríguez-Batista, R.; Gándara-Martínez, E.; Alcorta-García, A.; Martínez-Delgado, D.; Rodríguez-Castellanos, E.A.; Vázquez-Rodríguez, F.; Gómez-Rodríguez, C. Green Synthesis of Magnetic Nanoparticles of Iron Oxide Using Aqueous Extracts of Lemon Peel Waste and Its Application in Anti-Corrosive Coatings. *Materials (Basel)* **2022**, *15*, doi:10.3390/ma15238328.
120. Khan, M.Y.; Mangrich, A.S.; Schultz, J.; Grasel, F.S.; Mattoso, N.; Mosca, D.H. Green chemistry preparation of superparamagnetic nanoparticles containing Fe3O4 cores in biochar. *J. Anal. Appl. Pyrolysis* **2015**, *116*, 42–48, doi:10.1016/j.jaap.2015.10.008.
121. Sebastian, A.; Nangia, A.; Prasad, M.N.V. A green synthetic route to phenolics fabricated magnetite nanoparticles from coconut husk extract: Implications to treat metal contaminated water and heavy metal stress in Oryza sativa L. *J. Clean. Prod.* **2018**, *174*, 355–366, doi:10.1016/j.jclepro.2017.10.343.
122. Krishna Murthy, T.P.; Gowrishankar, B.S.; Krishna, R.H.; Chandraprabha, M.N.; Mathew, B.B. Magnetic modification of coffee husk hydrochar for adsorptive removal of methylene blue: Isotherms, kinetics and thermodynamic studies. *Environmental Chemistry and Ecotoxicology* **2020**, *2*, 205–212, doi:10.1016/j.enceco.2020.10.002.
123. Bishnoi, S.; Kumar, A.; Selvaraj, R. Facile synthesis of magnetic iron oxide nanoparticles using inedible Cynometra ramiflora fruit extract waste and their photocatalytic degradation of methylene blue dye. *Mater. Res. Bull.* **2018**, *97*, 121–127, doi:10.1016/j.materresbull.2017.08.040.

124. Izadiyan, Z.; Shameli, K.; Miyake, M.; Hara, H.; Mohamad, S.E.B.; Kalantari, K.; Taib, S.H.M.; Rasouli, E. Cytotoxicity assay of plant-mediated synthesized iron oxide nanoparticles using Juglans regia green husk extract. *Arabian Journal of Chemistry* **2018**, doi:10.1016/j.arabjc.2018.02.019.
125. Bano, S.; Nazir, S.; Nazir, A.; Munir, S.; Mahmood, T.; Afzal, M.; Ansari, F.L.; Mazhar, K. Microwave-assisted green synthesis of superparamagnetic nanoparticles using fruit peel extracts: surface engineering, T 2 relaxometry, and photodynamic treatment potential. *Int. J. Nanomedicine* **2016**, *11*, 3833–3848, doi:10.2147/IJN.S106553.
126. Venkateswarlu, S.; Rao, Y.S.; Balaji, T.; Prathima, B.; Jyothi, N.V.V. Biogenic synthesis of Fe3O4 magnetic nanoparticles using plantain peel extract. *Mater. Lett.* **2013**, *100*, 241–244, doi:10.1016/j.matlet.2013.03.018.
127. Yusefi, M.; Shameli, K.; Ali, R.R.; Pang, S.-W.; Teow, S.-Y. Evaluating Anticancer Activity of Plant-Mediated Synthesized Iron Oxide Nanoparticles Using Punica Granatum Fruit Peel Extract. *J. Mol. Struct* **2020**, *1204*, 127539, doi:10.1016/j.molstruc.2019.127539.
128. Yuvakkumar, R.; Hong, S.I. Green synthesis of spinel magnetite iron oxide nanoparticles. *AMR* **2014**, *1051*, 39–42, doi:10.4028/www.scientific.net/AMR.1051.39.
129. Areeshi, M.Y. Rice straw mediated green synthesis and characterization of iron oxide nanoparticles and its application to improve thermal stability of endoglucanase enzyme. *Int. J. Food Microbiol.* **2022**, *374*, 109722, doi:10.1016/j.ijfoodmicro.2022.109722.
130. Ehrampoush, M.H.; Miria, M.; Salmani, M.H.; Mahvi, A.H. Cadmium removal from aqueous solution by green synthesis iron oxide nanoparticles with tangerine peel extract. *J. Environ. Health Sci. Eng.* **2015**, *13*, 84, doi:10.1186/s40201-015-0237-4.
131. Prasad, Ch.; Gangadhara, S.; Venkateswarlu, P. Bio-inspired green synthesis of Fe3O4 magnetic nanoparticles using watermelon rinds and their catalytic activity. *Appl. Nanosci.* **2016**, *6*, 797–802, doi:10.1007/s13204-015-0485-8.
132. Buarki, F.; AbuHassan, H.; Al Hannan, F.; Henari, F.Z. Green Synthesis of Iron Oxide Nanoparticles Using Hibiscus rosa sinensis Flowers and Their Antibacterial Activity. *J. Nanotechnol.* **2022**, *2022*, 1–6, doi:10.1155/2022/5474645.
133. Demirezen, D.A.; Yılmaz, Ş.; Yılmaz, D.D.; Yıldız, Y.Ş. Green Synthesis of Iron Oxide Nanoparticles Using Ceratonia Siliqua L. Aqueous Extract: Optimization, Characterization, Stabilization and Evaluation of Its Antibacterial Activity Against Gram-Positive and Gram-Negative Bacteria. *Res. Sq.* **2022**, doi:10.21203/rs.3.rs-1302371/v1.
134. Mourdikoudis, S.; Pallares, R.M.; Thanh, N.T.K. Characterization techniques for nanoparticles: comparison and complementarity upon studying nanoparticle properties. *Nanoscale* **2018**, *10*, 12871–12934, doi:10.1039/c8nr02278j.
135. Kumar, A.; Dixit, C.K. Methods for characterization of nanoparticles. In *Advances in nanomedicine for the delivery of therapeutic nucleic acids*; Elsevier, 2017; pp. 43–58 ISBN 9780081005576.
136. Mohammed, L.; Gomaa, H.G.; Ragab, D.; Zhu, J. Magnetic nanoparticles for environmental and biomedical applications: A review. *Particuology* **2017**, *30*, 1–14, doi:10.1016/j.partic.2016.06.001.
137. Ali, A.; Shah, T.; Ullah, R.; Zhou, P.; Guo, M.; Ovais, M.; Tan, Z.; Rui, Y. Review on recent progress in magnetic nanoparticles: synthesis, characterization, and diverse applications. *Front. Chem.* **2021**, *9*, 629054, doi:10.3389/fchem.2021.629054.
138. Latham, A.H.; Wilson, M.J.; Schiffer, P.; Williams, M.E. TEM-induced structural evolution in amorphous Fe oxide nanoparticles. *J. Am. Chem. Soc.* **2006**, *128*, 12632–12633, doi:10.1021/ja064666q.
139. Sharma, D.; Ledwani, L.; Mehrotra, T.; Kumar, N.; Pervaiz, N.; Kumar, R. Biosynthesis of hematite nanoparticles using Rheum emodi and their antimicrobial and anticancerous effects in vitro. *J Photochem Photobiol B, Biol* **2020**, *206*, 111841, doi:10.1016/j.jphotobiol.2020.111841.
140. Ashraf, I.; Singh, N.B.; Agarwal, A. Green synthesis of iron oxide nanoparticles using Amla seed for methylene blue dye removal from water. *Materials Today: Proceedings* **2023**, *72*, 311–316, doi:10.1016/j.matpr.2022.07.404.
141. Calderón Bedoya, P.A.; Botta, P.M.; Bercoff, P.G.; Fanovich, M.A. Influence of the milling materials on the mechanochemical synthesis of magnetic iron oxide nanoparticles. *J Alloys Compd* **2023**, *939*, 168720, doi:10.1016/j.jallcom.2023.168720.
142. Gindaba, G.T.; Demsash, H.D.; Jayakumar, M. Green synthesis, characterization, and application of metal oxide nanoparticles for mercury removal from aqueous solution. *Environ. Monit. Assess.* **2022**, *195*, 9, doi:10.1007/s10661-022-10586-8.
143. Sasani, M.; Fataei, E.; Safari, R.; Nasehi, F.; Mosayyebi, M. Antimicrobial Potentials of Iron Oxide and Silver Nanoparticles Green-Synthesized in Fusarium solani. *Journal of Chemical Health Risks* **2023**.
144. Saleem, S.; Khan, M.S. Phyto-interactive impact of green synthesized iron oxide nanoparticles and Rhizobium pusense on morpho-physiological and yield components of greengram. *Plant Physiol. Biochem.* **2023**, *194*, 146–160, doi:10.1016/j.plaphy.2022.11.013.

145. Bansal, K.; Singh, J.; Dhaliwal, A.S. Green synthesis and characterization of superparamagnetic nanocomposite based on reduced graphene oxide/Fe_3O_4 prepared using leaf extract of *Azadirachta indica*. *Inorganic and Nano-Metal Chemistry* **2023**, 1–9, doi:10.1080/24701556.2023.2165688.
146. Nizam, A.; Warrier, V.G.; Devasia, J.; Ganganagappa, N. Magnetic iron oxide nanoparticles immobilized on microporous molecular sieves as efficient porous catalyst for photodegradation, transesterification and esterification reactions. *J. Porous Mater.* **2022**, *29*, 119–129, doi:10.1007/s10934-021-01150-9.
147. Afrouz, M.; Ahmadi-Nouraldinvand, F.; Elias, S.G.; Alebrahim, M.T.; Tseng, T.M.; Zahedian, H. Green synthesis of spermine coated iron nanoparticles and its effect on biochemical properties of Rosmarinus officinalis. *Sci. Rep.* **2023**, *13*, 775, doi:10.1038/s41598-023-27844-5.
148. Green synthesis and characterization of iron oxide nanoparticles using Coriandrum sativum L. leaf extract. *IJBB* **2022**, doi:10.56042/ijbb.v59i4.61913.
149. Rizvi, M.; Bhatia, T.; Gupta, R. Green & sustainable synthetic route of obtaining iron oxide nanoparticles using Hylocereus undantus (pitaya or dragon fruit). *Materials Today: Proceedings* **2022**, *50*, 1100–1106, doi:10.1016/j.matpr.2021.07.469.
150. Khan, Z.U.H.; Latif, S.; Abdulaziz, F.; Shah, N.S.; Imran, M.; Muhammad, N.; Iqbal, J.; Shahid, M.; Salam, M.A.; Khasim, S.; Khan, H.U. Photocatalytic response in water pollutants with addition of biomedical and anti-leishmanial study of iron oxide nanoparticles. *J Photochem Photobiol B, Biol* **2022**, *234*, 112544, doi:10.1016/j.jphotobiol.2022.112544.
151. K, V.; G, P.; S, M.; G, R.; S, S. Echinochloa frumentacea grains extract mediated synthesis and characterization of iron oxide nanoparticles: A greener nano drug for potential biomedical applications. *J. Drug Deliv. Sci. Technol.* **2022**, *76*, 103799, doi:10.1016/j.jddst.2022.103799.
152. Daniel, A.I.; Umar, M.B.; Tijani, O.J.; Muhammad, R. Antidiabetic potentials of green-synthesized alpha iron oxide nanoparticles using stem extract of Securidaca longipedunculata. *Int. Nano Lett.* **2022**, *12*, 281–293, doi:10.1007/s40089-022-00377-x.
153. Javad, S.; Maqsood, S.; Shah, A.A.; Singh, A.; Noor Shah, A.; Nawaz, M.; Bashir, M.A.; M.El Nashar, E.; A. Alghamdi, M.; F.El-kott, A.; Mosa, W.F.A. Iron nanoparticles mitigates cadmium toxicity in Triticum aestivum; Modulation of antioxidative defense system and physiochemical characteristics. *Journal of King Saud University - Science* **2023**, *35*, 102498, doi:10.1016/j.jksus.2022.102498.
154. Prabhu, P.; Rao, M.; Murugesan, G.; Narasimhan, M.K.; Varadavenkatesan, T.; Vinayagam, R.; Lan Chi, N.T.; Pugazhendhi, A.; Selvaraj, R. Synthesis, characterization and anticancer activity of the green-synthesized hematite nanoparticles. *Environ. Res.* **2022**, *214*, 113864, doi:10.1016/j.envres.2022.113864.
155. Green synthesis of iron oxide nanoparticles by using ficus carica leaf extract and its antioxidant activity. *Biointerface Res. Appl. Chem.* **2021**, *12*, 2108–2116, doi:10.33263/BRIAC122.21082116.
156. (2) (PDF) Green Synthesis-Mediated Iron Oxide Nanoparticles using. Available online: https://www.researchgate.net/publication/371416474_Green_Synthesis-Mediated_Iron_Oxide_Nanoparticles_using (accessed on 19 September 2023).
157. Hazel, D.; Gobi, N. One-Pot Facile Green Synthesis of Iron Oxide Nanoparticles Using Aqueous Stem Extract of Amaranthus Campestris and Comparison of its Characteristics with Chemically Synthesized Iron Oxide Nanoparticles. *Res. Sq.* **2022**, doi:10.21203/rs.3.rs-2213450/v1.
158. Kiwumulo, H.F.; Muwonge, H.; Ibingira, C.; Lubwama, M.; Kirabira, J.B.; Ssekitoleko, R.T. Green synthesis and characterization of iron-oxide nanoparticles using Moringa oleifera: a potential protocol for use in low and middle income countries. *BMC Res. Notes* **2022**, *15*, 149, doi:10.1186/s13104-022-06039-7.
159. Ananthi, S.; Kavitha, M.; Kumar, E.R.; Balamurugan, A.; Al-Douri, Y.; Alzahrani, H.K.; Keshk, A.A.; Habeebullah, T.M.; Abdel-Hafez, S.H.; El-Metwaly, N.M. Natural tannic acid (green tea) mediated synthesis of ethanol sensor based Fe3O4 nanoparticles: Investigation of structural, morphological, optical properties and colloidal stability for gas sensor application. *Sensors and Actuators B: Chemical* **2022**, *352*, 131071, doi:10.1016/j.snb.2021.131071.
160. Saad AlGarni, T.; Ali, M.H.H.; Al-Mohaimeed, A.M. Green biosynthesis of Fe3O4 nanoparticles using Chlorella vulgaris extract for enhancing degradation of 2,4 dinitrophenol. *Journal of King Saud University - Science* **2023**, *35*, 102426, doi:10.1016/j.jksus.2022.102426.
161. Shahwan, T.; Abu Sirriah, S.; Nairat, M.; Boyacı, E.; Eroğlu, A.E.; Scott, T.B.; Hallam, K.R. Green synthesis of iron nanoparticles and their application as a Fenton-like catalyst for the degradation of aqueous cationic and anionic dyes. *Chemical Engineering Journal* **2011**, *172*, 258–266, doi:10.1016/j.cej.2011.05.103.
162. Lesiak, B.; Rangam, N.; Jiricek, P.; Gordeev, I.; Tóth, J.; Kövér, L.; Mohai, M.; Borowicz, P. Surface study of fe3o4 nanoparticles functionalized with biocompatible adsorbed molecules. *Front. Chem.* **2019**, *7*, 642, doi:10.3389/fchem.2019.00642.
163. Adhikari, A.; Chhetri, K.; Acharya, D.; Pant, B.; Adhikari, A. Green Synthesis of Iron Oxide Nanoparticles Using Psidium guajava L. Leaves Extract for Degradation of Organic Dyes and Anti-microbial Applications. *Catalysts* **2022**, *12*, 1188, doi:10.3390/catal12101188.

164. Mundekkad, D.; Alex, A.V. Analysis of structural and biomimetic characteristics of the green-synthesized Fe3O4 nanozyme from the fruit peel extract of Punica granatum. *Chem. Pap.* **2022**, *76*, 3863–3878, doi:10.1007/s11696-022-02130-2.
165. Birusanti, A.B.; Espenti, C.S.; Mala, S. Plant-Extract-Assisted Eco-friendly synthesis of Iron oxide nanoparticles using cape gooseberry Extract and their Antibacterial study. *Res. Sq.* **2022**, doi:10.21203/rs.3.rs-1954952/v1.
166. Roychoudhury, P.; Golubeva, A.; Dąbek, P.; Pryshchepa, O.; Sagandykova, G.; Pomastowski, P.; Gloc, M.; Dobrucka, R.; Kurzydłowski, K.; Buszewski, B.; Witkowski, A. Study on Biogenic Spindle-Shaped Iron-Oxide Nanoparticles by Pseudostaurosira trainorii in Field of Laser Desorption/Ionization Applications. *Int. J. Mol. Sci.* **2022**, *23*, doi:10.3390/ijms231911713.
167. Vorontsov, A.V.; Tsybulya, S.V. Influence of nanoparticles size on XRD patterns for small monodisperse nanoparticles of cu^{0} and tio$_{2}$ anatase. *Ind. Eng. Chem. Res.* **2018**, *57*, 2526–2536, doi:10.1021/acs.iecr.7b04480.
168. Weirich, T.E.; Zou, X.; Ramlau, R.; Simon, A.; Cascarano, G.L.; Giacovazzo, C.; Hovmöller, S. Structures of nanometre-size crystals determined from selected-area electron diffraction data. *Acta Crystallogr, A, Found Crystallogr* **2000**, *56*, 29–35, doi:10.1107/s0108767399009605.
169. Charron, G.; Hühn, D.; Perrier, A.; Cordier, L.; Pickett, C.J.; Nann, T.; Parak, W.J. On the use of pH titration to quantitatively characterize colloidal nanoparticles. *Langmuir* **2012**, *28*, 15141–15149, doi:10.1021/la302570s.
170. Aksu Demirezen, D.; Yılmaz, Ş.; Demirezen Yılmaz, D.; Yıldız, Y.Ş. Green synthesis of iron oxide nanoparticles using *Ceratonia siliqua L.* aqueous extract: improvement of colloidal stability by optimizing synthesis parameters, and evaluation of antibacterial activity against Gram-positive and Gram-negative bacteria. *IJMR* **2022**, *113*, 849–861, doi:10.1515/ijmr-2022-0037.
171. Mohamad Ebrahimzadeh Sepasgozar, S.; Mohseni, S.; Feyzizadeh, B.; Morsali, A. Eco-Friendly Synthesis of Magnetic Iron Oxide Nanoparticles Using Achillea Nobilis Extract and Evaluation of Their Antioxidant and Antibacterial properties. *Journal of Food Biosciences and Technology* **2022**.
172. Zhang, Y.; Yang, M.; Portney, N.G.; Cui, D.; Budak, G.; Ozbay, E.; Ozkan, M.; Ozkan, C.S. Zeta potential: a surface electrical characteristic to probe the interaction of nanoparticles with normal and cancer human breast epithelial cells. *Biomed. Microdevices* **2008**, *10*, 321–328, doi:10.1007/s10544-007-9139-2.
173. Schwegmann, H.; Feitz, A.J.; Frimmel, F.H. Influence of the zeta potential on the sorption and toxicity of iron oxide nanoparticles on S. cerevisiae and E. coli. *J. Colloid Interface Sci.* **2010**, *347*, 43–48, doi:10.1016/j.jcis.2010.02.028.
174. Sakulkhu, U.; Mahmoudi, M.; Maurizi, L.; Salaklang, J.; Hofmann, H. Protein corona composition of superparamagnetic iron oxide nanoparticles with various physico-chemical properties and coatings. *Sci. Rep.* **2014**, *4*, 5020, doi:10.1038/srep05020.
175. Samrot, A.V.; Senthilkumar, P.; Rashmitha, S.; Veera, P.; Sahithya, C.S. Azadirachta indica influenced biosynthesis of super-paramagnetic iron-oxide nanoparticles and their applications in tannery water treatment and X-ray imaging. *J. Nanostruct. Chem.* **2018**, *8*, 343–351, doi:10.1007/s40097-018-0279-0.
176. Wypij, M.; Czarnecka, J.; Świecimska, M.; Dahm, H.; Rai, M.; Golinska, P. Synthesis, characterization and evaluation of antimicrobial and cytotoxic activities of biogenic silver nanoparticles synthesized from Streptomyces xinghaiensis OF1 strain. *World J. Microbiol. Biotechnol.* **2018**, *34*, 23, doi:10.1007/s11274-017-2406-3.
177. Ghamipoor, S.; Fayyazi, F.; Bahadorikhalili, S. Phytochemical synthesis of silver nanoparticles using anthemis nobilis extract and its antibacterial activity. *Zeitschrift für Physikalische Chemie* **2020**, *234*, 531–540, doi:10.1515/zpch-2018-1288.
178. Gu, H.; Chen, X.; Chen, F.; Zhou, X.; Parsaee, Z. Ultrasound-assisted biosynthesis of CuO-NPs using brown alga Cystoseira trinodis: Characterization, photocatalytic AOP, DPPH scavenging and antibacterial investigations. *Ultrason. Sonochem.* **2018**, *41*, 109–119, doi:10.1016/j.ultsonch.2017.09.006.
179. Wiesner, M.R.; Lowry, G.V.; Casman, E.; Bertsch, P.M.; Matson, C.W.; Di Giulio, R.T.; Liu, J.; Hochella, M.F. Meditations on the ubiquity and mutability of nano-sized materials in the environment. *ACS Nano* **2011**, *5*, 8466–8470, doi:10.1021/nn204118p.
180. Matinise, N.; Fuku, X.G.; Kaviyarasu, K.; Mayedwa, N.; Maaza, M. ZnO nanoparticles via Moringa oleifera green synthesis: Physical properties & mechanism of formation. *Appl. Surf. Sci.* **2017**, *406*, 339–347, doi:10.1016/j.apsusc.2017.01.219.
181. Titus, D.; James Jebaseelan Samuel, E.; Roopan, S.M. Nanoparticle characterization techniques. In *Green synthesis, characterization and applications of nanoparticles*; Elsevier, 2019; pp. 303–319 ISBN 9780081025796.
182. Niraimathee, V.A.; Subha, V.; Ravindran, R.S.E.; Renganathan, S. Green synthesis of iron oxide nanoparticles from Mimosa pudica root extract. *IJESD* **2016**, *15*, 227, doi:10.1504/IJESD.2016.077370.
183. Bouafia, A.; Laouini, S.E. Green synthesis of iron oxide nanoparticles by aqueous leaves extract of Mentha Pulegium L.: Effect of ferric chloride concentration on the type of product. *Mater. Lett.* **2020**, *265*, 127364, doi:10.1016/j.matlet.2020.127364.

184. Aziz, W.J.; Abid, M.A.; Kadhim, D.A.; Mejbel, M.K. Synthesis of iron oxide (β-fe2 o3) nanoparticles from Iraqi grapes extract and its biomedical application. *IOP Conf. Ser.: Mater. Sci. Eng.* **2020**, *881*, 012099, doi:10.1088/1757-899X/881/1/012099.
185. Zhang, C.; Firestein, K.L.; Fernando, J.F.S.; Siriwardena, D.; von Treifeldt, J.E.; Golberg, D. Recent progress of in situ transmission electron microscopy for energy materials. *Adv. Mater.* **2020**, *32*, e1904094, doi:10.1002/adma.201904094.
186. Inkson, B.J. Scanning electron microscopy (SEM) and transmission electron microscopy (TEM) for materials characterization. In *Materials characterization using nondestructive evaluation (NDE) methods*; Elsevier, 2016; pp. 17–43 ISBN 9780081000403.
187. Zheng, H.; Meng, Y.S.; Zhu, Y. Frontiers of *in situ* electron microscopy. *MRS Bull.* **2015**, *40*, 12–18, doi:10.1557/mrs.2014.305.
188. Munawer, U.; Raghavendra, V.B.; Ningaraju, S.; Krishna, K.L.; Ghosh, A.R.; Melappa, G.; Pugazhendhi, A. Biofabrication of gold nanoparticles mediated by the endophytic Cladosporium species: Photodegradation, in vitro anticancer activity and in vivo antitumor studies. *Int. J. Pharm.* **2020**, *588*, 119729, doi:10.1016/j.ijpharm.2020.119729.
189. Jamdagni, P.; Khatri, P.; Rana, J.S. Green synthesis of zinc oxide nanoparticles using flower extract of Nyctanthes arbor-tristis and their antifungal activity. *Journal of King Saud University - Science* **2016**, doi:10.1016/j.jksus.2016.10.002.
190. Cheng, Y.; Zhang, L.; Zhang, Q.; Li, J.; Tang, Y.; Delmas, C.; Zhu, T.; Winter, M.; Wang, M.-S.; Huang, J. Understanding all solid-state lithium batteries through in situ transmission electron microscopy. *Materials Today* **2021**, *42*, 137–161, doi:10.1016/j.mattod.2020.09.003.
191. Vijayaraghavan, K.; Ashokkumar, T. Plant-mediated biosynthesis of metallic nanoparticles: A review of literature, factors affecting synthesis, characterization techniques and applications. *Journal of Environmental Chemical Engineering* **2017**, *5*, 4866–4883, doi:10.1016/j.jece.2017.09.026.
192. Patravale, V.; Dandekar, P.; Jain, R. Characterization techniques for nanoparticulate carriers. In *Nanoparticulate Drug Delivery*; Elsevier, 2012; pp. 87–121 ISBN 9781907568985.
193. Yadav, V.K.; Fulekar, M.H. Biogenic synthesis of maghemite nanoparticles (γ-Fe2O3) using Tridax leaf extract and its application for removal of fly ash heavy metals (Pb, Cd). *Materials Today: Proceedings* **2018**, *5*, 20704–20710, doi:10.1016/j.matpr.2018.06.454.
194. Fouladi-Fard, R.; Aali, R.; Mohammadi-Aghdam, S.; Mortazavi-derazkola, S. The surface modification of spherical ZnO with Ag nanoparticles: A novel agent, biogenic synthesis, catalytic and antibacterial activities. *Arabian Journal of Chemistry* **2022**, *15*, 103658, doi:10.1016/j.arabjc.2021.103658.
195. Senthil Kumar, K.; Moorthy Babu, S.; Bhagavannarayana, G. Study of the influence of dopants on the crystalline perfection of ferroelectric glycine phosphite single crystals using high-resolution X-ray diffraction analysis. *J. Appl. Crystallogr.* **2011**, *44*, 313–318, doi:10.1107/S0021889811005140.
196. Malinov, S.; Sha, W.; Guo, Z.; Tang, C.C.; Long, A.E. Synchrotron X-ray diffraction study of the phase transformations in titanium alloys. *Materials Characterization* **2002**, *48*, 279–295, doi:10.1016/S1044-5803(02)00286-3.
197. Monshi, A.; Foroughi, M.R.; Monshi, M.R. Modified Scherrer Equation to Estimate More Accurately Nano-Crystallite Size Using XRD. *WJNSE* **2012**, *02*, 154–160, doi:10.4236/wjnse.2012.23020.
198. Bhattacharjee, S. DLS and zeta potential - What they are and what they are not? *J. Control. Release* **2016**, *235*, 337–351, doi:10.1016/j.jconrel.2016.06.017.
199. Stetefeld, J.; McKenna, S.A.; Patel, T.R. Dynamic light scattering: a practical guide and applications in biomedical sciences. *Biophys. Rev.* **2016**, *8*, 409–427, doi:10.1007/s12551-016-0218-6.
200. Kaszuba, M.; McKnight, D.; Connah, M.T.; McNeil-Watson, F.K.; Nobbmann, U. Measuring sub nanometre sizes using dynamic light scattering. *J. Nanopart. Res.* **2008**, *10*, 823–829, doi:10.1007/s11051-007-9317-4.
201. Riedl, J.C.; Sarkar, M.; Fiuza, T.; Cousin, F.; Depeyrot, J.; Dubois, E.; Mériguet, G.; Perzynski, R.; Peyre, V. Design of concentrated colloidal dispersions of iron oxide nanoparticles in ionic liquids: Structure and thermal stability from 25 to 200 °C. *J. Colloid Interface Sci.* **2022**, *607*, 584–594, doi:10.1016/j.jcis.2021.08.017.
202. Slavin, Y.N.; Asnis, J.; Häfeli, U.O.; Bach, H. Metal nanoparticles: understanding the mechanisms behind antibacterial activity. *J. Nanobiotechnology* **2017**, *15*, 65, doi:10.1186/s12951-017-0308-z.
203. Sihem, L.; Hanine, D.; Faiza, B. Antibacterial Activity of α-Fe2O3 and α-Fe2O3@Ag Nanoparticles Prepared by Urtica Leaf Extract. *Nanotechnol. Russ.* **2020**, *15*, 198–203, doi:10.1134/S1995078020020135.
204. Li, D.; Shen, M.; Xia, J.; Shi, X. Recent developments of cancer nanomedicines based on ultrasmall iron oxide nanoparticles and nanoclusters. *Nanomedicine (Lond)* **2021**, *16*, 609–612, doi:10.2217/nnm-2021-0033.
205. AlMatar, M.; Makky, E.A.; Var, I.; Koksal, F. The Role of Nanoparticles in the Inhibition of Multidrug-Resistant Bacteria and Biofilms. *Curr. Drug Deliv.* **2018**, *15*, 470–484, doi:10.2174/1567201815666171207163504.
206. Lee, C.; Kim, J.Y.; Lee, W.I.; Nelson, K.L.; Yoon, J.; Sedlak, D.L. Bactericidal effect of zero-valent iron nanoparticles on Escherichia coli. *Environ. Sci. Technol.* **2008**, *42*, 4927–4933, doi:10.1021/es800408u.

207. Aisida, S.O.; Batool, A.; Khan, F.M.; Rahman, L.; Mahmood, A.; Ahmad, I.; Zhao, T.; Maaza, M.; Ezema, F.I. Calcination induced PEG-Ni-ZnO nanorod composite and its biomedical applications. *Mater. Chem. Phys* **2020**, *255*, 123603, doi:10.1016/j.matchemphys.2020.123603.
208. Touati, D. Iron and oxidative stress in bacteria. *Arch. Biochem. Biophys.* **2000**, *373*, 1–6, doi:10.1006/abbi.1999.1518.
209. Padmavathy, N.; Vijayaraghavan, R. Enhanced bioactivity of ZnO nanoparticles-an antimicrobial study. *Sci. Technol. Adv. Mater.* **2008**, *9*, 035004, doi:10.1088/1468-6996/9/3/035004.
210. Jayanthi, S.A. The influence of PEG 20,000 concentration on the size control and magnetic properties of functionalized bio-compatible magnetic nanoparticles | Abstract. *Der Pharma Chemica* **2013**.
211. Armijo, L.M.; Wawrzyniec, S.J.; Kopciuch, M.; Brandt, Y.I.; Rivera, A.C.; Withers, N.J.; Cook, N.C.; Huber, D.L.; Monson, T.C.; Smyth, H.D.C.; Osiński, M. Antibacterial activity of iron oxide, iron nitride, and tobramycin conjugated nanoparticles against Pseudomonas aeruginosa biofilms. *J. Nanobiotechnology* **2020**, *18*, 35, doi:10.1186/s12951-020-0588-6.
212. Li, Y.; Yang, D.; Wang, S.; Li, C.; Xue, B.; Yang, L.; Shen, Z.; Jin, M.; Wang, J.; Qiu, Z. The Detailed Bactericidal Process of Ferric Oxide Nanoparticles on E. coli. *Molecules* **2018**, *23*, doi:10.3390/molecules23030606.
213. Gabrielyan, L.; Hovhannisyan, A.; Gevorgyan, V.; Ananyan, M.; Trchounian, A. Antibacterial effects of iron oxide (Fe3O4) nanoparticles: distinguishing concentration-dependent effects with different bacterial cells growth and membrane-associated mechanisms. *Appl. Microbiol. Biotechnol.* **2019**, *103*, 2773–2782, doi:10.1007/s00253-019-09653-x.
214. Yu, J.; Zhang, W.; Li, Y.; Wang, G.; Yang, L.; Jin, J.; Chen, Q.; Huang, M. Synthesis, characterization, antimicrobial activity and mechanism of a novel hydroxyapatite whisker/nano zinc oxide biomaterial. *Biomed. Mater.* **2014**, *10*, 015001, doi:10.1088/1748-6041/10/1/015001.
215. Kohanski, M.A.; DePristo, M.A.; Collins, J.J. Sublethal antibiotic treatment leads to multidrug resistance via radical-induced mutagenesis. *Mol. Cell* **2010**, *37*, 311–320, doi:10.1016/j.molcel.2010.01.003.
216. Guittat, L.; Alberti, P.; Rosu, F.; Van Miert, S.; Thetiot, E.; Pieters, L.; Gabelica, V.; De Pauw, E.; Ottaviani, A.; Riou, J.-F.; Mergny, J.-L. Interactions of cryptolepine and neocryptolepine with unusual DNA structures. *Biochimie* **2003**, *85*, 535–547, doi:10.1016/s0300-9084(03)00035-x.
217. Morones, J.R.; Elechiguerra, J.L.; Camacho, A.; Holt, K.; Kouri, J.B.; Ramírez, J.T.; Yacaman, M.J. The bactericidal effect of silver nanoparticles. *Nanotechnology* **2005**, *16*, 2346–2353, doi:10.1088/0957-4484/16/10/059.
218. Nel, A.E.; Mädler, L.; Velegol, D.; Xia, T.; Hoek, E.M.V.; Somasundaran, P.; Klaessig, F.; Castranova, V.; Thompson, M. Understanding biophysicochemical interactions at the nano-bio interface. *Nat. Mater.* **2009**, *8*, 543–557, doi:10.1038/nmat2442.
219. Javanbakht, T.; Laurent, S.; Stanicki, D.; Wilkinson, K.J. Relating the Surface Properties of Superparamagnetic Iron Oxide Nanoparticles (SPIONs) to Their Bactericidal Effect towards a Biofilm of Streptococcus mutans. *PLoS ONE* **2016**, *11*, e0154445, doi:10.1371/journal.pone.0154445.
220. Al-Shabib, N.A.; Husain, F.M.; Ahmed, F.; Khan, R.A.; Khan, M.S.; Ansari, F.A.; Alam, M.Z.; Ahmed, M.A.; Khan, M.S.; Baig, M.H.; Khan, J.M.; Shahzad, S.A.; Arshad, M.; Alyousef, A.; Ahmad, I. Low Temperature Synthesis of Superparamagnetic Iron Oxide (Fe3O4) Nanoparticles and Their ROS Mediated Inhibition of Biofilm Formed by Food-Associated Bacteria. *Front. Microbiol.* **2018**, *9*, 2567, doi:10.3389/fmicb.2018.02567.
221. Kolen'ko, Y.V.; Bañobre-López, M.; Rodríguez-Abreu, C.; Carbó-Argibay, E.; Sailsman, A.; Piñeiro-Redondo, Y.; Cerqueira, M.F.; Petrovykh, D.Y.; Kovnir, K.; Lebedev, O.I.; Rivas, J. Large-Scale Synthesis of Colloidal Fe_3O_4 Nanoparticles Exhibiting High Heating Efficiency in Magnetic Hyperthermia. *J. Phys. Chem. C* **2014**, *118*, 8691–8701, doi:10.1021/jp500816u.
222. Li, W.; Wei, W.; Wu, X.; Zhao, Y.; Dai, H. The antibacterial and antibiofilm activities of mesoporous hollow Fe3O4 nanoparticles in an alternating magnetic field. *Biomater. Sci.* **2020**, *8*, 4492–4507, doi:10.1039/d0bm00673d.
223. Madubuonu, N.; Aisida, S.O.; Ali, A.; Ahmad, I.; Zhao, T.-K.; Botha, S.; Maaza, M.; Ezema, F.I. Biosynthesis of iron oxide nanoparticles via a composite of Psidium guavaja-Moringa oleifera and their antibacterial and photocatalytic study. *J Photochem Photobiol B, Biol* **2019**, *199*, 111601, doi:10.1016/j.jphotobiol.2019.111601.
224. Patra, J.K.; Ali, M.S.; Oh, I.-G.; Baek, K.-H. Proteasome inhibitory, antioxidant, and synergistic antibacterial and anticandidal activity of green biosynthesized magnetic Fe3O4 nanoparticles using the aqueous extract of corn (Zea mays L.) ear leaves. *Artif. Cells Nanomed. Biotechnol.* **2017**, *45*, 349–356, doi:10.3109/21691401.2016.1153484.
225. Ebrahiminezhad, A.; Zare, M.; Kiyanpour, S.; Berenjian, A.; Niknezhad, S.V.; Ghasemi, Y. Biosynthesis of xanthangum-coated INPs by using *Xanthomonas campestris*. *IET nanobiotechnol.* **2018**, *12*, 254–258, doi:10.1049/iet-nbt.2017.0199.
226. Majeed, S.; Abdullah, M.S. bin; Nanda, A.; Ansari, M.T. In vitro study of the antibacterial and anticancer activities of silver nanoparticles synthesized from Penicillium brevicompactum (MTCC-1999). *Journal of Taibah University for Science* **2016**, *10*, 614–620, doi:10.1016/j.jtusci.2016.02.010.

227. Sathishkumar, G.; Logeshwaran, V.; Sarathbabu, S.; Jha, P.K.; Jeyaraj, M.; Rajkuberan, C.; Senthilkumar, N.; Sivaramakrishnan, S. Green synthesis of magnetic Fe3O4 nanoparticles using Couroupita guianensis Aubl. fruit extract for their antibacterial and cytotoxicity activities. *Artif. Cells Nanomed. Biotechnol.* **2018**, *46*, 589–598, doi:10.1080/21691401.2017.1332635.
228. Yoonus, J.; Resmi, R.; Beena, B. Evaluation of antibacterial and anticancer activity of green synthesized iron oxide (α-Fe2O3) nanoparticles. *Materials Today: Proceedings* **2021**, *46*, 2969–2974, doi:10.1016/j.matpr.2020.12.426.
229. Al-Karagoly, H.; Rhyaf, A.; Naji, H.; Albukhaty, S.; AlMalki, F.A.; Alyamani, A.A.; Albaqami, J.; Aloufi, S. Green synthesis, characterization, cytotoxicity, and antimicrobial activity of iron oxide nanoparticles using *Nigella sativa* seed extract. *Green Processing and Synthesis* **2022**, *11*, 254–265, doi:10.1515/gps-2022-0026.
230. Mirza, A.U.; Kareem, A.; Nami, S.A.A.; Khan, M.S.; Rehman, S.; Bhat, S.A.; Mohammad, A.; Nishat, N. Biogenic synthesis of iron oxide nanoparticles using Agrewia optiva and Prunus persica phyto species: Characterization, antibacterial and antioxidant activity. *J Photochem Photobiol B, Biol* **2018**, *185*, 262–274, doi:10.1016/j.jphotobiol.2018.06.009.
231. Muhammad, W.; Khan, M.A.; Nazir, M.; Siddiquah, A.; Mushtaq, S.; Hashmi, S.S.; Abbasi, B.H. Papaver somniferum L. mediated novel bioinspired lead oxide (PbO) and iron oxide (Fe2O3) nanoparticles: In-vitro biological applications, biocompatibility and their potential towards HepG2 cell line. *Mater. Sci. Eng. C Mater. Biol. Appl.* **2019**, *103*, 109740, doi:10.1016/j.msec.2019.109740.
232. Qasim, S.; Zafar, A.; Saif, M.S.; Ali, Z.; Nazar, M.; Waqas, M.; Haq, A.U.; Tariq, T.; Hassan, S.G.; Iqbal, F.; Shu, X.-G.; Hasan, M. Green synthesis of iron oxide nanorods using Withania coagulans extract improved photocatalytic degradation and antimicrobial activity. *J Photochem Photobiol B, Biol* **2020**, *204*, 111784, doi:10.1016/j.jphotobiol.2020.111784.
233. Ali, K.; Ahmed, B.; Khan, M.S.; Musarrat, J. Differential surface contact killing of pristine and low EPS Pseudomonas aeruginosa with Aloe vera capped hematite (α-Fe2O3) nanoparticles. *J Photochem Photobiol B, Biol* **2018**, *188*, 146–158, doi:10.1016/j.jphotobiol.2018.09.017.
234. Arasu, M.V.; Arokiyaraj, S.; Viayaraghavan, P.; Kumar, T.S.J.; Duraipandiyan, V.; Al-Dhabi, N.A.; Kaviyarasu, K. One step green synthesis of larvicidal, and azo dye degrading antibacterial nanoparticles by response surface methodology. *J Photochem Photobiol B, Biol* **2019**, *190*, 154–162, doi:10.1016/j.jphotobiol.2018.11.020.
235. Bachheti, R.K.; Konwarh, R.; Gupta, V.; Husen, A.; Joshi, A. Green synthesis of iron oxide nanoparticles: cutting edge technology and multifaceted applications. In *Nanomaterials and plant potential*; Husen, A., Iqbal, M., Eds.; Springer International Publishing: Cham, 2019; pp. 239–259 ISBN 978-3-030-05568-4.
236. Parveen, S.; Wani, A.H.; Shah, M.A.; Devi, H.S.; Bhat, M.Y.; Koka, J.A. Preparation, characterization and antifungal activity of iron oxide nanoparticles. *Microb. Pathog.* **2018**, *115*, 287–292, doi:10.1016/j.micpath.2017.12.068.
237. Asghar, M.A.; Zahir, E.; Shahid, S.M.; Khan, M.N.; Asghar, M.A.; Iqbal, J.; Walker, G. Iron, copper and silver nanoparticles: Green synthesis using green and black tea leaves extracts and evaluation of antibacterial, antifungal and aflatoxin B 1 adsorption activity. *LWT* **2018**, *90*, 98–107, doi:10.1016/j.lwt.2017.12.009.
238. Henam, S.D.; Ahmad, F.; Shah, M.A.; Parveen, S.; Wani, A.H. Microwave synthesis of nanoparticles and their antifungal activities. *Spectrochim. Acta A Mol. Biomol. Spectrosc.* **2019**, *213*, 337–341, doi:10.1016/j.saa.2019.01.071.
239. Nehra, P.; Chauhan, R.P.; Garg, N.; Verma, K. Antibacterial and antifungal activity of chitosan coated iron oxide nanoparticles. *Br. J. Biomed. Sci.* **2018**, *75*, 13–18, doi:10.1080/09674845.2017.1347362.
240. Soliman, G.M. Nanoparticles as safe and effective delivery systems of antifungal agents: Achievements and challenges. *Int. J. Pharm.* **2017**, *523*, 15–32, doi:10.1016/j.ijpharm.2017.03.019.
241. Dorostkar, R.; Ghalavand, M.; Nazarizadeh, A.; Tat, M.; Hashemzadeh, M.S. Anthelmintic effects of zinc oxide and iron oxide nanoparticles against Toxocara vitulorum. *Int. Nano Lett.* **2017**, *7*, 157–164, doi:10.1007/s40089-016-0198-3.
242. hassan, ahmed; Ramdan, M.; S.F. A, O.; Elkabawy, L. In vitro anthelmintic effects of iron oxide and zinc oxide nanoparticles against Fasciola Spp. in Dakhla Oasis, Egypt. *Benha Veterinary Medical Journal* **2021**, *41*, 144–147, doi:10.21608/bvmj.2021.83038.1442.
243. Kannan, D.; Yadav, N.; Ahmad, S.; Namdev, P.; Bhattacharjee, S.; Lochab, B.; Singh, S. Pre-clinical study of iron oxide nanoparticles fortified artesunate for efficient targeting of malarial parasite. *EBioMedicine* **2019**, *45*, 261–277, doi:10.1016/j.ebiom.2019.06.026.
244. Abidi, H.; Ghaedi, M.; Rafiei, A.; Jelowdar, A.; Salimi, A.; Asfaram, A.; Ostovan, A. Magnetic solid lipid nanoparticles co-loaded with albendazole as an anti-parasitic drug: Sonochemical preparation, characterization, and in vitro drug release. *J. Mol. Liq.* **2018**, *268*, 11–18, doi:10.1016/j.molliq.2018.06.116.
245. Ain, Q. ul; Islam, A.; Nadhman, A.; Yasinzai, M. Comparative analysis of chemically and biologically synthesized iron oxide nanoparticles against Leishmania tropica. *BioRxiv* **2019**, doi:10.1101/829408.

246. Mohamed, H.E.A.; Afridi, S.; Khalil, A.T.; Ali, M.; Zohra, T.; Salman, M.; Ikram, A.; Shinwari, Z.K.; Maaza, M. Bio-redox potential of Hyphaene thebaica in bio-fabrication of ultrafine maghemite phase iron oxide nanoparticles (Fe2O3 NPs) for therapeutic applications. *Materials Science and Engineering: C* **2020**, *112*, 110890, doi:10.1016/j.msec.2020.110890.
247. Chakravarty, M.; Vora, A. Nanotechnology-based antiviral therapeutics. *Drug Deliv. Transl. Res.* **2021**, *11*, 748–787, doi:10.1007/s13346-020-00818-0.
248. Abate, C.; Carnamucio, F.; Giuffrè, O.; Foti, C. Metal-Based Compounds in Antiviral Therapy. *Biomolecules* **2022**, *12*, 933, doi:10.3390/biom12070933.
249. Galdiero, S.; Falanga, A.; Vitiello, M.; Cantisani, M.; Marra, V.; Galdiero, M. Silver nanoparticles as potential antiviral agents. *Molecules* **2011**, *16*, 8894–8918, doi:10.3390/molecules16108894.
250. Shahabadi, N.; Khorshidi, A.; Zhaleh, H.; Kashanian, S. Synthesis, characterization, cytotoxicity and DNA binding studies of Fe 3 O 4 @SiO 2 nanoparticles coated by an antiviral drug lamivudine. *J. Drug Deliv. Sci. Technol.* **2018**, *46*, 55–65, doi:10.1016/j.jddst.2018.04.016.
251. Kumar, R.; Sahoo, G.C.; Chawla-Sarkar, M.; Nayak, M.K.; Trivedi, K.; Rana, S.; Pandey, K.; Das, V.; Topno, R.; Das, P. Antiviral effect of Glycine coated Iron oxide nanoparticles iron against H1N1 influenza A virus. *Int. J. Infect. Dis.* **2016**, *45*, 281–282, doi:10.1016/j.ijid.2016.02.622.
252. Kumar, R.; Nayak, M.; Sahoo, G.C.; Pandey, K.; Sarkar, M.C.; Ansari, Y.; Das, V.N.R.; Topno, R.K.; Bhawna; Madhukar, M.; Das, P. Iron oxide nanoparticles based antiviral activity of H1N1 influenza A virus. *J. Infect. Chemother.* **2019**, *25*, 325–329, doi:10.1016/j.jiac.2018.12.006.
253. Gour, A.; Jain, N.K. Advances in green synthesis of nanoparticles. *Artif. Cells Nanomed. Biotechnol.* **2019**, *47*, 844–851, doi:10.1080/21691401.2019.1577878.